

UNIVERSITY OF OKLAHOMA
GRADUATE COLLEGE

NEW IMPLICATION OF SHORT CIRCUIT ANALYSIS IN ASSESSING IMPACT
OF RENEWABLE ENERGY RESOURCES ON SYSTEM STRENGTH OF A
POWER GRID

A DISSERTATION
SUBMITTED TO THE GRADUATE FACULTY
in partial fulfillment of the requirements for the
Degree of
DOCTOR OF PHILOSOPHY

By
MILAD JAVADI
Norman, Oklahoma
2017

NEW IMPLICATION OF SHORT CIRCUIT ANALYSIS IN ASSESSING IMPACT
OF RENEWABLE ENERGY RESOURCES ON SYSTEM STRENGTH OF A
POWER GRID

A DISSERTATION APPROVED FOR THE
SCHOOL OF ELECTRICAL AND COMPUTER ENGINEERING

BY

Dr. John N. Jiang, Chair

Dr. Joseph P. Havlicek

Dr. Choon Yik Tang

Dr. Krishnaiyan Thulasiraman

Dr. Theodore B. Trafalis

© Copyright by MILAD JAVADI 2017
All Rights Reserved.

Dedicated to my immediate family

Acknowledgments

First of all, I would like to thank my academic advisor Dr. John N. Jiang for his ubiquitous support during my graduate studies. It was a great opportunity for me to work with him, and I am grateful for his invaluable advices.

I would like to thank the Oklahoma Gas & Electric Corp. (OG&E) for providing me with the opportunity of doing several projects for them during my graduate studies.

Many thanks go to my colleagues in the Electricity and Energy Risk and Reliability Research Laboratory, University of Oklahoma, specifically Dr. Di Wu for his support, consultations and contributions in my research and projects.

I would like to thank the faculty members at the University of Oklahoma for their continuous support during my graduate studies. In particular, I would like to express my gratitude to Dr. John N. Jiang, Dr. Joseph P. Havlicek, Dr. Choon Yik Tang, Dr. Krishnaiyan Thulasiraman and Dr. Theodore B. Trafalis for serving on my committee and providing constructive comments and guidelines.

At the end, I would like to thank my immediate family for their kind support and encouragement.

Table of Contents

Acknowledgments	iv
List of Tables	ix
List of Figures.....	x
Abstract.....	xiii
Chapter 1: Introduction.....	1
1.1 Importance of understanding impact of renewable energy resource on power grid operation.....	1
1.2 System strength evaluation for assessment of impacts of renewable energy resources on power grid operation	3
1.3 Overview of contributions of this dissertation	5
Chapter 2: Theoretical Foundation of System Strength Evaluation	8
2.1 Short Circuit Ratio (SCR)	8
2.2 Strong and weak points of interconnection	10
2.3 Limitations of basic short circuit ratio.....	12
2.4 Existing modified measures for system strength evaluation	14
2.4.1 Weighted Short Circuit Ratio (WSCR)	14
2.4.2 Composite Short Circuit Ratio (CSCR)	15
2.4.3 Limitations of existing SCR-based measures.....	17
Chapter 3: A New Measure for System Strength Evaluation Based on Power Grid Structure	19
3.1 Theoretical foundation: relation between voltage stability and system strength	20

3.1.1 Voltage stability analysis in a power grid with single inverter-based generation unit	20
3.1.2 Relation between static voltage stability and system strength	23
3.2 Site Dependent Short Circuit Ratio (SDSCR) for system strength evaluation ..	24
3.2.1 Study of voltage stability in a power grid with multiple inverter-based generation units	24
3.2.2 SDSCR measure and features	28
Chapter 4: Particular Features and Applications of SDSCR Measure	29
4.1 Particular privileges of SDSCR over existing methods	29
4.2 Power grid structural analysis using SDSCR	32
4.3 System strength evaluation for integration of renewable energy resources	34
4.4 Implementation and validation of SDSCR measure.....	36
4.4.1 Approach of validation study	36
4.4.2 Validation study using WSCC 9-bus system.....	39
4.5 Improved system strength evaluation based on more accurate forecast of renewable power generation.....	42
4.5.1 Estimation of wind farms power generation	43
4.5.2 Estimation of solar PV plants power generation	44
Chapter 5: A SAS-based Algorithm for Estimation of Actual Power Curve of a Wind Farm/Turbine Based on Operation Data.....	45
5.1 Introduction to wind power curve estimation.....	45
4.2 Model for estimation of power curves and error reduction	51
4.2.1 Data-Driven Model for Estimation of Power Curves.....	51

4.2.2 Errors Involved in Estimated Model	52
4.3 A SAS-based algorithm for estimating wind farm/turbine power curve.....	55
4.3.1 Fitting a piece-wise linear model to dataset	56
4.3.2 Data Cleaning for Bias Error Reduction	60
Chapter 6: Estimation of Solar PV Plants Power Generation Drops Based on Clouds Distribution.....	67
6.1 Solar power generation.....	67
6.2 Reliability challenge of solar power generation.....	69
6.3 Impact of clouds distribution on solar power generation drops	70
6.4 Impact of clouds distribution and solar power generation drops on system strength	72
6.5 Estimation of clouds distribution.....	74
6.5.1 Definition of cloud modes from power system operation perspective	76
6.5.2. An approach of estimating clouds distribution.....	77
6.5.3 Approach Illustration using simulation study.....	79
6.6 More precise evaluation of system strength for solar PV plants	83
Chapter 7: Identifying Combination of Weakest Points of Interconnection Using Structural Analysis	85
7.1 Weakest point of interconnection	85
7.2 Challenge of identifying weakest combination of points of interconnection....	88
7.3 Impact of Grid Structure and Topological Locations on System Strength	90
7.4 Identifying weakest combination of points of interconnection grid structure analysis	93

7.5 Criteria for identification of the weakest combination of points of interconnection based on grid structure.....	96
Chapter 8: Simulation Studies	100
8.1 SDSCR Measure Case Study.....	100
8.2 Wind Turbine Power Curve Estimation Case Study	106
Summary and Concluding Remarks	113
References	116

List of Tables

Table 1. System strength evaluation results (WSCC 9-bus system)	41
Table 2. Relation between clouds modes and quartile numbers	79
Table 3. Sample of central Oklahoma weather dataset	81
Table 4. Results of clouds distribution forecast	81
Table 5. Solar PV plants generation capacities	101
Table 7. Results of iterative non-linear parameter estimation for recursive outlier elimination.....	109
Table 8. Number of eliminated outliers in each recursion	110

List of Figures

Figure 1. ERCOT transmission grid and Panhandle area	2
Figure 2. An AC power grid interconnected to a inverter-based system (renewable resource)	9
Figure 3. Thevenin equivalent of power grid shown in Figure 2	9
Figure 4. Threshold of basic SCR for estimating the system strength	10
Figure 5. A power grid with multiple renewable resources	14
Figure 6. Threshold of WSCR for system strength evaluation	15
Figure 7. Creating a composite bus for the CSCR measure	16
Figure 8. Threshold of WSCR for system strength evaluation	16
Figure 9. An AC power grid with single inverter-based generation unit	20
Figure 10. Equivalence of an AC power grid with single inverter-based generation unit	20
Figure 11. An AC power grid with multiple inverter-based generation units	25
Figure 12. Equivalence of an AC power grid with multiple inverter-based generation units	26
Figure 13. Flowchart of validation study	37
Figure 14. P-V curve with important points	38
Figure 15. WSCC 9-bus system with two renewable energy resources	40
Figure 16. P-V curve at bus 3	40
Figure 17. A typical wind turbine power curve with the critical points	46
Figure 18. A wind turbine power generation-wind speed raw data	49
Figure 19. Scatterplot of a dataset with 2 correlated variables s and p	57

Figure 20. A piece-wise linear model fitted to the dataset	60
Figure 21. Flowchart of the recursive algorithm for power curve estimation.....	64
Figure 22. A mock power curve on which the order of outlier elimination for each recursion of the algorithm is shown	65
Figure 23. Arial and close views of a 110MW solar PV plant in the state of Nevada ...	68
Figure 24. Relation between system strength and the cloud distribution.....	73
Figure 25. Pictures (a)-(f) show clouds distribution over the United States	76
Figure 26. Map of Oklahoma state with the 9 weather stations	80
Figure 27. Clouds distribution over state of Oklahoma obtained from satellite data....	82
Figure 28. Solar irradiance on February 23, 2015	82
Figure 29. IEEE 118-bus power transmission system with three renewable resources interconnected to different locations in two scenarios	87
Figure 30. Stressed scenarios of renewable resource integration study	89
Figure 31. Node-edge model of transmission system of a large-scale power grid.....	94
Figure 32. Plot of vectors associated with points of interconnection.....	95
Figure 33. Structural impact on system strength (vector angle).....	97
Figure 34. Structural impact on system strength (vector magnitude)	98
Figure 35. Flowchart of recursive procedure for identifying weakest combinations	99
Figure 36. Excerpt of a large-scale power grid with three renewable resources.....	101
Figure 37. P-V Curve at bus interconnected to renewable resource #1	102
Figure 38. Results of system strength evaluation for POI #1	103
Figure 39. Results of system strength evaluation at POIs 2 and 3	104
Figure 40. Power curver after first recursion.....	111

Figure 41. Power curve after second recursion 111

Figure 42. Final power curve piece-wise linear model 112

Abstract

The increasing penetration of renewable resources raised a new challenge in power system planning and operation to maintain system reliability. Several serious operational issues may take place when significant amount of renewable power is penetrated into a weak power grid. Short circuit ratio with some modifications has been used to study system strength. The existing short circuit ratio calculation measures have some limitations, and do not consider the realistic electrical connections among multiple renewable resources. The system strength evaluation results obtained from using these measures may not accurately reflect the impact of the interactions among multiple renewable resources at different locations on the system strength. To take the realistic electrical connections among multiple renewable resources into consideration of system strength evaluation study, in this dissertation, a novel Site Dependent Short Circuit Ratio (SDSCR) measure is proposed by analyzing the relationship between the system strength and static voltage stability.

The proposed measure evaluates the system strength based on the power grid structural characteristics and considering the amount of renewable power generation at a point of interconnection. It can be used for various studies concerning system strength evaluation, such as identifying weakest combination of points of interconnection. As another application of the proposed measure, an approach is developed to identify the weakest combination of points of interconnection through structural analysis.

In order to improve the system strength evaluation studies using the proposed measure, this dissertation also proposed an algorithm for more accurate estimation of wind power generation, and an approach for estimation of solar PV power generation drops.

An algorithm for more accurate estimation of wind power generation: an accurate estimation of power curves is essential for assessing the actual output characteristics of a wind farm. The power curve can be estimated using the measured power output data comprising wind power generation and wind speed. However, these measured data are generally ill-distributed due to significant number of outliers, which impose a serious bias challenging estimation of power curves. In this dissertation, an intelligent algorithm is proposed for estimating power curves using the measured data while minimizing modeling and bias errors caused by outliers in the data. Particularly, the proposed algorithm is designed based on statistical analysis software (SAS) package in order to facilitate the analysis of a big dataset.

An approach for estimation of solar PV power generation drops: it becomes more and more clear that dramatic variation of solar power generation will impact the grid reliability and voltage stability. Particularly, in a high penetration scenario, estimation of solar power generation drops is very important for reliability management and operation. In this dissertation, the impact of clouds distribution on solar irradiance, and thus the solar power generation drops are investigated. Then an approach is developed to forecast the clouds distribution using weather data. The approach utilizes time-series weather data including several weather parameters around the solar PV plant of interest to forecast the clouds distribution, and therefore sudden solar power generation drops.

Chapter 1: Introduction

1.1 Importance of understanding impact of renewable energy resource on power grid operation

Power grids are undergoing significant change of generation resources. High penetration of renewable energy resources is changing the system characteristics and rises new challenges in transmission operation/planning and power system operation about maintaining system reliability and voltage stability. By interconnecting a large number of renewable resources, such as wind farms, solar PV and battery storage plants, power grid becomes weaker and more vulnerable at specific locations (i.e., weak points of interconnection/buses). The weak points of system are more in risk of serious undesired operational problems, such as high/low voltage and VAR inadequacy issues, voltage flickers, reliability problems, or even voltage instability.

Renewables are commonly interconnected to the remote areas in the distribution or transmission systems, which are electrically far from the AC power grid and synchronous generators. From power grid structure perspective, these points of interconnection are weak and voltage stability problems are likely to happen at these locations when inadequate VAR support (reactive power) is provided. Figure 1 shows the Panhandle area in the Texas power transmission grid, which is a competitive renewable energy zones, [1]. As it can be seen this area with serval renewable resources is weakly connected to the rest of the AC power grid through a few high voltage transmission lines. It increases the electrical distance with the renewable resources and the main power grid,

so that sudden variations of renewable power generation and VAR sufficiency problems will be difficultly compensated by the synchronous generators.

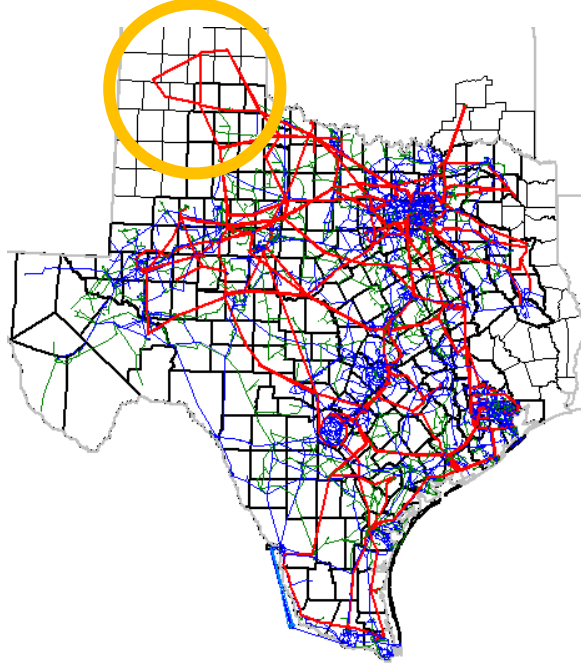


Figure 1. ERCOT transmission grid and Panhandle area

Moreover, renewables are interconnected to the power grid by power inverter¹ controllers. They are fast-acting solid state devices that increase the sensitivity of voltage to reactive power support. Marginal variations in VAR support would result in noticeable oscillations in voltage profile of the point of interconnection. Such voltage oscillations may cause wide-spread voltage stability problems, or even loss of generation synchronism and/or critical damages to power electronics equipment associated with the renewable resources, [2]–[4]. In addition, renewable power generation includes several important uncertainties, which may jeopardize the system reliability in high penetration

¹ An inverter, or converter or renewable resource inverter, converts the variable direct current (DC) output of a non-synchronous generation unit into a utility frequency alternating current (AC) that can be fed into a power grid or used by a local, off-grid electrical network.

scenarios. For example, it is known that clouds movement and the level of solar irradiance are highly correlated, which implies solar irradiance may also suddenly vary at various geographical locations due to clouds movement. Solar irradiance plays a critical role in operating condition of the solar PV plants. The operating condition is characterized by the rate of solar power generation change and the distribution of output level that both may affect the power grid reliability. As another example, wind power generation is constrained by nondeterministic variations of wind speed. Sudden variations of wind speed over specific periods of times/dates may result in serious high/low voltage problems at the point of interconnection of the wind farm to the power grid.

All these operational challenges require to be monitored and assessed by the power system/renewable operators to understand the possible impacts of renewable resources on power grid operating condition and stability status, such as voltage stability, VAR adequacy, transmission system strength at the points of interconnection, etc.

1.2 System strength evaluation for assessment of impacts of renewable energy resources on power grid operation

System strength can be used as a measure to evaluate how integration of renewable resources may affect the power grid stability and operating condition. System strength is defined as the ability of the power grid to remain stable and maintain the quality of load service (e.g., voltage stability) during and following significant variations in outputs of non-synchronous/solid-state devices, such as renewable resources. More specifically, it takes into consideration particular important parameters such as, power grid short circuit capacity, electrical distance between a renewable resource and the AC

power grid and amount of renewable power generation at the point of interconnection to assess the impact of renewables on power grid.

The system strength is commonly measured through Short Circuit Ratio (SCR) analysis. SCR has traditionally several conventional applications in power system studies, such as, power system protection equipment calibration, relays configuration and threshold setting, DC link (DC transmission lines) interconnection to AC power grid, synchronous machines characteristics determination, [5]. Recently SCR has been used as a measurement to evaluate the strength of the power grid at the points of interconnection of renewable resources, [6]–[9]. However, the commonly used SCR calculation method has some limitations and ignores the impact of other renewable energy resources on the point of interconnection of interest. This may result in overly-optimistic estimation of system strength at the points of interconnection of renewable resources, or even misleading results. To take into account the effect this impact, some new methods were developed, namely Composite Short Circuit Ratio (CSCR) by General Electric Corp. (GE) and Weighted Short Circuit Ratio, [10], [11], and (WSCR) by the Electric Reliability Council of Texas (ERCOT), [12], [13]. The CSCR and WSCR methods do not take into consideration the real electrical connections among renewable energy resources, which plays an important role in estimation of actual system strength at each point of the interconnection.

In addition to having an appropriate method to measure the system strength, accurate and realistic forecast of renewable power generation plays a critical role in system strength evaluation. If the amount of renewable power generation at a point of interconnection is overestimated/underestimated, consequently the results of system

strength evaluation studies will not be accurate enough, and this may result in inaccurate decisions making in transmission operation and/or transmission planning. All the existing SCR-based methods of system strength evaluation normally consider the full-capacity of renewable resources to be in or out of service. Using the full-capacity (i.e., assuming a plant is generating either 0MW or at its maximum MW capacity) might be too conservative that can result in misleading or even unrealistic results for high penetration scenarios. If the realistic operating condition of a renewable resource can be used instead of its full-capacity, the system strength would be more accurately evaluated. The realistic operating condition can be estimated if we have high-resolution information about the distribution of output level and dramatic variation of renewable power generation.

1.3 Overview of contributions of this dissertation

This dissertation is focused on development of an enhanced SCR-based method, which evaluates the system strength based on more accurate forecast of renewable power generations (i.e., wind and solar power). This method is developed through studying the relation between system strength and static voltage stability and power grid structure properties. Hence, it provides the system strength evaluation results in terms of proximity to voltage instability limit, and takes into account the effect of interactions among multiple renewable energy resources at various locations on the system strength according to the real electrical connections among renewables interconnected to a power grid.

For more accurate forecast of renewable power generation, two comprehensive studies are performed, which result in (1) proposing an algorithm to accurately forecast

the power generation of wind farms based real-world operation data, and (2) developing a method for accurate forecast of solar power generation and sudden drops of generation based on weather condition and clouds distribution. More precisely, these methods forecast the renewable power generation as follows:

- 1) A SAS-based algorithm for estimation of actual power curve of a wind turbine/farm based on operation data,

An accurate estimation of power curves is essential for assessing the actual output characteristics and power generation of a wind farm, as the power curve provided by the manufacturer changes after several years of operation. The power curve can be estimated using the measured power output data comprising wind power generation and wind speed. However, these measured data are generally ill-distributed due to significant number of outliers, which impose a serious bias challenging estimation of power curves. In this research, an intelligent algorithm is proposed for estimating power curves using the measured data while minimizing modeling and bias errors caused by outliers in the data. Particularly, the proposed algorithm is designed based on statistical analysis software (SAS) package in order to facilitate the analysis of a big dataset. The effectiveness and practical application of the proposed algorithm is demonstrated using real-world weather and wind farm operation datasets.

- 2) A method for investigation of impact of clouds on output level and variation of solar PV generation for system strength evaluation,

Importance of having realistic operating condition of renewable resources was the motivation to conduct research on estimating the realistic operating condition of

solar PV plants, which can be utilized for more accurate system strength evaluation. In this research, the knowledge of weather condition is used to forecast the clouds distribution and utilizing that information for improved forecast of solar irradiance and power generation.

More specifically, the time-series weather data is used to train an Artificial Neural Network (ANN) model that forecasts the solar irradiance. The model's associated forecast errors are considered as a measure to define several cloud modes which can be used to estimate the realistic solar PV plant operating condition including sudden drops of power generation. Having knowledge of realistic operating condition is beneficial for more accurate system strength evaluation. The validity of the study is being verified by visualizing the satellite cloud data provided by the National Oceanic and Atmospheric Administration (NOAA), [14], and National Weather Center (NWC), [15].

Chapter 2: Theoretical Foundation of System Strength Evaluation

In this chapter, the theoretical foundation of system strength evaluation and Short Circuit Ratio (SCR) are presented. More specifically, first SCR is defined and its applications are introduced, then the existing SCR-based measures for system strength evaluation are reviewed and their limitations are discussed, and finally an enhanced new measure is proposed, based on power grid structural properties, for system strength evaluation.

2.1 Short Circuit Ratio (SCR)

The system strength of an AC power grid has a significant impact on the AC/DC system interactions. Hence it is very beneficial to have a simple means of measuring and comparing the relative system strength of an AC power grid. The SCR has evolved as such a measure. It is defined as the ratio of “short circuit capacity” of an AC power grid to the “MW power injection” that takes place at point i .

$$SCR_i = \frac{|S_{AC,i}|}{P_{DC,i}} = \frac{|V_i|^2}{P_{DC,i}} \cdot \frac{1}{|Z_i|} \quad (1)$$

where $|S_{AC,i}|$ is the short-circuit capacity of the system at bus i ; $P_{DC,i}$ is the rated amount power injected to bus i ; $|V_i|$ is the voltage magnitude at bus i ; and $|Z_i|$ is the magnitude of the Thevenin equivalent impedance at bus i .

The power grid shown in Figure 2 is interconnected to a DC system (e.g., a inverter-based generation resource like a solar PV plant) can be represented with its Thevenin equivalent shown in Figure 3.

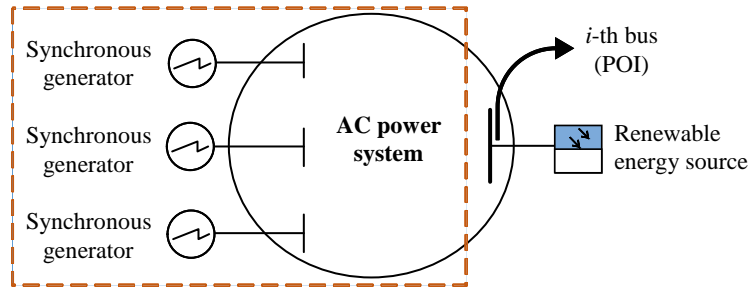


Figure 2. An AC power grid interconnected to a inverter-based system (renewable resource)

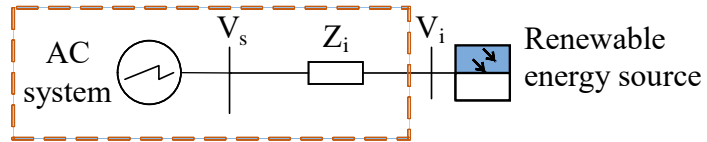


Figure 3. Thevenin equivalent of power grid shown in Figure 2

SCR (also called basic SCR) provides the inherent system strength of an AC power grid at bus i . Hence it has several conventional applications in power system studies, such as, protection equipment calibration, relays configuration and threshold setting studies, DC link interconnection to the AC power grid, synchronous machine characteristics determination.

Recently the concept of SCR is being used for a new application, which is evaluating the system strength at the point of interconnection of inverter-based generation units (e.g., renewable resources). It is defined the ratio of “short circuit capacity” of an AC power grid to the “MW renewable power injection” at the point of interconnection i . The value of SCR shows if the power grid has the enough strength (capability) of absorbing a certain amount of renewable power without serious operational problems. With respect to the value of SCR a point of interconnection can be identified as strong,

weak, or very weak. Figure 4 shows the threshold of (basic) SCR for estimating the system strength. For example, if the value of the basic SCR_i is equal to 3.6, the point of interconnection i is identified as a strong point, in opposite if SCR_i is equal to 1.87, the point of interconnection i is identified as a very weak point for interconnection of a DC link/system or a renewable resource.

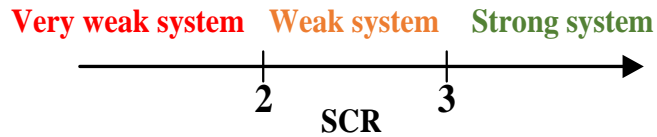


Figure 4. Threshold of basic SCR for estimating the system strength

2.2 Strong and weak points of interconnection

The SCR measure is used to measure the system strength at a specific point of interconnection. Based on the value of SCR and the threshold shown in Figure 4, a point of interconnection is identified as strong, weak or very weak.

- Weak and very weak points of interconnection

Weak points are interconnection are problematic load or transfer buses with the lowest system strength values. Sudden variation of inverter-based power generation likely causes serious operational problems, [5] such as,

- Dynamic overvoltage: When there is an interruption in the inverter-based power transfer, VAR absorption of converters drops to zero. At a weak point of interconnection, the resulting increase in the AC voltage can be more than necessary due to shunt capacitors and harmonic filters. It may result in damaging the residential/industrial pieces of equipment.

- Voltage stability issues: When an inverter-based generation unit is interconnected to a weak point of an AC power grid, the DC/AC voltages are very sensitive to changes in variations of load, especially on the inverter-side. An increase in the power generation on the inverter side, the AC voltage at the point of interconnection can be significantly dropped. Thus, secure increase of power generation should be very small and control of voltage and recovery from disturbances would be more challenging. This sensitivity increases with large amounts of shunt capacitors. In such a system, the DC controls may contribute to the voltage instability occurrence by responding to a reduction in the AC voltage at the point of interconnection.
- Harmonic resonance: Most of the issues related to harmonic resonance are because of parallel resonance between capacitors, filters and the AC power grid at lower harmonics. Capacitors lower the natural resonant frequencies, while machines and transmission/distribution lines tend to increase the frequency. If several capacitors are added, the natural frequency seen by the commutation bus may drop to the 4th, 3rd or even 2nd harmonic. If a resonance at one these frequencies happens, there may be a high impedance parallel resonance between the machines/lines and the capacitors on the commutation bus. This can become a serious problem from the transient stability perspective, since avoiding the low-order harmonic resonances is a key point to reduce transient voltages.
- Voltage flicker: At a weak point of interconnection, switching the shunt capacitors and reactors causes undesirable significant voltage variations in the

vicinity of compensation devices. The transient voltage flicker, due to frequently switched reactive support devices, increases with high penetration of inverter-based power generation.

A very weak point of interconnection (bus) is extremely sensitive to variations of load, and a sudden change of load/generation at such a bus may result in voltage flicker, voltage instability or other serious operational difficulties.

- Strong points of interconnection

They are those points of interconnection with the highest system strengths (i.e., SCR values bigger than 3). The voltage of a strong point of interconnection/bus is less sensitive to variations of load. Moreover, they are electrically close to the Thevenin equivalence of the AC power grid and the effect of sudden changes of inverter-based generation/load at these buses can be compensated by the synchronous generators. Thus, they are considered as appropriate candidates for future integration of DC links and/or inverter-based generation resources, such as wind farms and/or solar PV plants.

2.3 Limitations of basic short circuit ratio

The basic SCR measure has an important limitation that may result in overestimation of system at the point of interconnection of interest. It ignores the impact of other inverter-based power injections (or renewable resources) on the system strength at the point of interconnection of interest. In other words, it does not take the interactions among renewable resources into consideration of system strength evaluation. When the

inverter-based power injections are electrically close, they interact with each other and reduce the system strength at their points of interconnection. Thus, the SCR measure may overestimate the system strength at the points of interconnection due to ignorance of impact of other inverter-based power injections/renewable resources. This measure works for evaluating the system strength in the power grids interconnected to single inverter-based generators.

To further illustrate the importance of taking the interaction among inverter-based power injections into consideration of system strength evaluation, let's evaluate the system strength at a particular bus of the power grid shown in Figure 5. In this power grid, there are several synchronous generators with Automatic Voltage Regulators (AVR) and capability of providing sufficient VAR to maintain the voltage schedule², and four renewable resources (i.e., plants *B*, *C*, *D* and *E*). If we are planning to integrate a new solar PV plant to point of interconnection *A* and evaluate the system strength at this point using the basic SCR, the system strength would be equal to the ratio of short circuit capacity of the AC power grid to the full-capacity of the solar PV plant of interest at point *A*. The result of this system strength evaluation is obtained with respect to inverter-based power generation only at point *A*, and the impacts of other inverter-based power generations are ignored. It is known that interconnection of more inverter-based power generators makes the power grid weaker at the points of interconnection. Thus, the result of system strength evaluation using the basic SCR is expected to be overestimated. Extensive simulation studies have also confirmed that results may not accurate or may be even misleading.

² Voltage schedule is a set of secure practical values for each nominal voltage level that should be maintained within a certain range to maintain voltage stability of the generation zones.

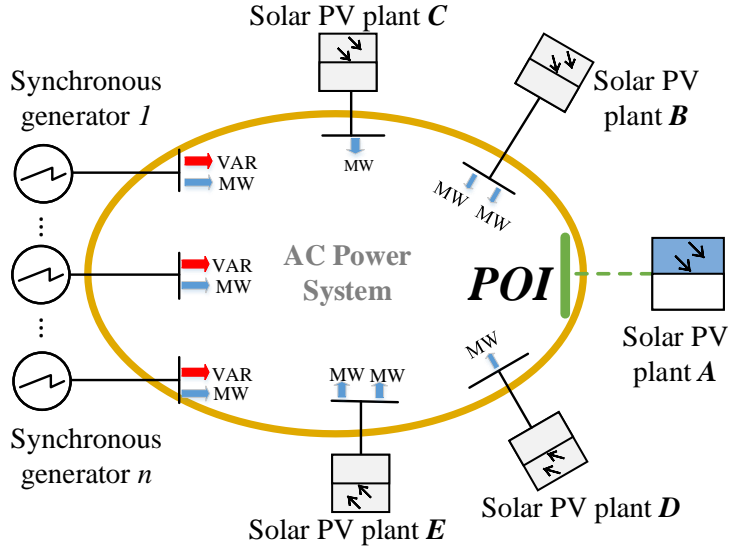


Figure 5. A power grid with multiple renewable resources

2.4 Existing modified measures for system strength evaluation

In order to overcome the limitation of SCR measure for system strength evaluation, which is taking into account the effect of interactions among inverter-based generation units, several studies have been performed and a few measures were developed, [7], [13], [16]–[20]. Two measures that are mostly accepted by the power industry are Composite Short Circuit Ratio (CSCR) developed by GE, and Weighted Short Circuit Ratio (WSCR) developed by ERCOT.

2.4.1 Weighted Short Circuit Ratio (WSCR)

ERCOT developed this measure of system strength evaluation to take into account the effect of interactions among several inverter-based generation units, [13]. In development of this measure it is assumed that all the inverter-based generation units are electrically close to each other. Based on this assumption, it uses the weighted average of the short

circuit capacity of all inverter-based generation units to evaluate the system strength as follows,

$$WSCR = \frac{\text{Weighted } S_{SC}}{\sum_i^N P_{i,RE}} \quad (2)$$

$$= \frac{(\sum_i^N S_{i,SC} \times P_{i,RE}) / \sum_i^N P_{i,RE}}{\sum_i^N P_{i,RE}} = \frac{\sum_i^N S_{i,SC} \times P_{i,RE}}{(\sum_i^N P_{i,RE})^2} \quad (3)$$

where $S_{i,SC}$ is the short circuit capacity at bus i before interconnection of inverter-based generation unit i ; $P_{i,RE}$ is the MW rating of inverter-based generation unit i to be connected; N is the number of inverter-based generation units fully interacting with each other, and i is the inverter-based generation unit index.

This measure has a specific threshold to evaluate the system strength of a power grid. Based on this threshold, if the value of the WSCR is more than 1.5, the system is strong, otherwise the system is weak for a given amount of inverter-based power generation. Figure 6 shows the threshold of the WSCR,

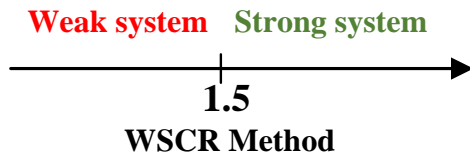


Figure 6. Threshold of WSCR for system strength evaluation

2.4.2 Composite Short Circuit Ratio (CSCR)

This measure is developed by GE to consider the interactions among the inverter-based generation units, [10]. In development of this measure, it is also assumed that all the inverter-based generation units are electrically very close to each other such that they

can be considered connected to a particular bus. It uses this assumption to tie all inverter-based generation unit buses to create a “composite” bus as shown in Figure 7.

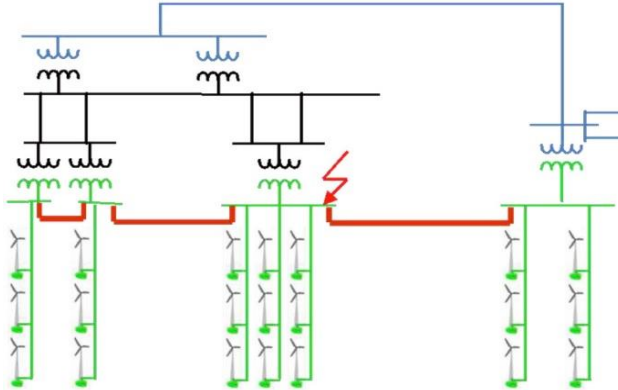


Figure 7. Creating a composite bus for the CSCR measure

To evaluate the system strength, the SCR is then calculated at the composite bus as follows,

$$CSCR = \frac{\text{Short circuit ratio at the composite bus}}{\text{Total MW rating of all inverter-based generators}} \quad (4)$$

This measure also has a specific threshold to evaluate the system strength of a power grid as it is shown in Figure 8. Based on this threshold, a system with a CSCR above about 2.5 to 3 is considered strong. The point of interconnection of the inverter-based generation unit should not have control instability issues. CSCR below about 1.7 to 1.5 is considered weak; and CSCR below 1.0 would likely require mitigation, either at the plant through control tuning or by strengthening the system.

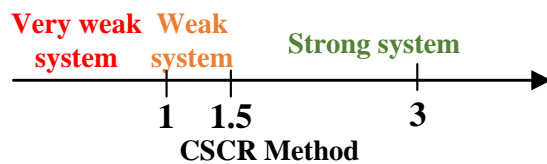


Figure 8. Threshold of WSCR for system strength evaluation

2.4.3 Limitations of existing SCR-based measures

The basic SCR, WSCR and CSCR can be used for system strength evaluation; however, they have some limitations that may result in overestimated/underestimated and/or inaccurate results. More specifically, each measure has the following limitations,

- Short Circuit Ratio (SCR)

It does not take the interactions among inverter-based generation units into consideration of system strength evaluation. When inverter-based generation units are electrically close, they interact with each other. In other words, they lower the system strength at each other points of interconnection. In such cases, the basic SCR may overestimate the system strength at the points of interconnection of inverter-based generation units.

- Composite Short Circuit Ratio (CSCR) and Weighted Short Circuit Ratio (WSCR)

Both of these measures have some limitations that the major ones are as follows,

- These two measures are developed based on the assumption of having all inverter-based generation units electrically very close to each other. In a power system with high penetration of renewable resources and Distributed Generation units (DG), the inverter-based generation units are not all electrically close to each other; however, they impact the system strength at each other's points of interconnection.

- They do not explain the relation between system strength and voltage stability,

These measures only evaluate the system strength for the power grid to

identify the system as a weak or a strong system, and do not provide any meaningful information on the status of voltage stability. The results of system strength evaluation obtained from them do not show the distance between the current operating condition of the system and the voltage instability limit. As VAR sufficiency and voltage stability are very important concerns in operation of inverter-based generation units, it is very beneficial to evaluate the system strength in terms of proximity to voltage stability limit.

- Inability of providing a particular system strength evaluation at each point of interconnection/bus,

These two measures evaluate the system strength for the whole power grid not at each point of interconnection. However, extensive simulation studies show that system strength is different at each point of interconnection due to particular structural characteristics of the power grid.

A SCR-based measure would provide more informative and meaningful information on the system strength of a power grid if it can:

- consider the interaction among all the interconnected inverter-based generation units,
- provide a particular system strength evaluation for each point of interconnection,
- explain the system strength in terms of proximity to voltage stability limit.

Chapter 3: A New Measure for System Strength Evaluation Based on Power Grid Structure

In this chapter, a new SCR-based measure is proposed that evaluates the system strength at each point of interconnection through analyzing the power grid structural properties and the relation between system strength and static voltage stability. The proposed measure can evaluate system strength in terms of the distance to voltage instability limit. Moreover, it takes into account the effect of interactions among inverter-based generation units at different locations with respect to the real electrical connections among the inverter-based generation units. The practical applicability and efficiency of the proposed measure are demonstrated by comparing its system strength evaluation results with the results obtained from the basic SCR, CSCR, and WSCR on the IEEE 39-bus system. In addition, the foundation and potentials of the proposed measure for power grid structural analysis are discussed.

In order to overcome the limitations of the existing measures for the system strength evaluation, Site Dependent Short Circuit Ratio (SDSCR) is proposed as an enhanced measure over the existing ones. Development of the proposed measure includes the following studies:

- 1) Analyzing and deriving the sufficient and necessary condition of voltage instability occurrence,
- 2) Deriving the relation between voltage instability and system strength (SCR) in a power grid interconnected to single inverter-based generation unit.

- 3) Deriving the relation between voltage instability and system strength in a power grid with multiple interconnected inverter-based generation units.
- 4) Defining the enhanced SCR-based measure for system strength evaluation based on the relation found in the 3rd step and power grid structural properties.

3.1 Theoretical foundation: relation between voltage stability and system strength

3.1.1 Voltage stability analysis in a power grid with single inverter-based generation unit

In a power grid with single inverter-based generation unit shown in Figure 9, its voltage stability³ can be studied in an equivalent two-bus power system as shown in Figure 10.

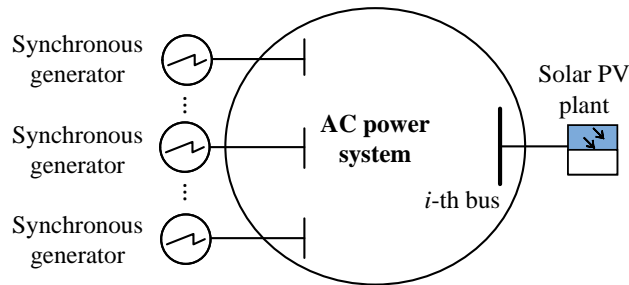


Figure 9. An AC power grid with single inverter-based generation unit

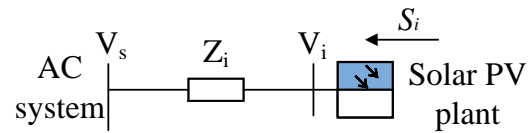


Figure 10. Equivalence of an AC power grid with single inverter-based generation unit

³ Voltage stability is the ability of a power grid to maintain steady acceptable voltages at all buses under normal operating condition and after being subjected to disturbances.

In the equivalent system, the power grid network equation can be represented as follows,

$$\frac{V_i - V_s}{Z_i} = I_i = \left(\frac{S_i}{V_i} \right)^* \quad (5)$$

where S_i is the complex power injected into bus i ; V_i and V_s are the voltages at buses i and s ; and Z_i is the Thevenin equivalent impedance at bus i .

According to (5), we can derive the voltage stability boundary condition at bus i .

More specifically, we first rewrite (5) as the following equation,

$$Z_i S_i^* = |V_i|^2 - V_s V_i^* \quad (6)$$

Let $Z_i S_i^* = a - jb$ where a and b are two real numbers. Based on (6), a and b can be represented as,

$$a = |V_i|^2 - |V_s| |V_i| \cos \theta_{si} \quad (7)$$

$$b = |V_s| |V_i| \sin \theta_{si} \quad (8)$$

where $|V_s|$ and $|V_i|$ are the magnitudes of voltages V_s and V_i ; $\theta_{si} = \theta_s - \theta_i$ is the angular difference of voltages V_s and V_i .

When the voltage magnitude $|V_s|$ is constant, a and b are the functions of $|V_i|$ and θ_{si} . That is,

$$a = f_1(|V_i|, \theta_{si}) = |V_i|^2 - |V_s| |V_i| \cos \theta_{si} \quad (9)$$

$$b = f_2(|V_i|, \theta_{si}) = |V_s| |V_i| \sin \theta_{si} \quad (10)$$

The Jacobian matrix of $f = [f_1, f_2]^T$ can be represented as,

$$J = \begin{bmatrix} \frac{\partial f_1}{\partial |V_i|} & \frac{\partial f_1}{\partial \theta_{si}} \\ \frac{\partial f_2}{\partial |V_i|} & \frac{\partial f_2}{\partial \theta_{si}} \end{bmatrix} \quad (11)$$

$$= \begin{bmatrix} 2|V_i| - |V_s| \cos \theta_{si} & |V_s| |V_i| \sin \theta_{si} \\ |V_s| \sin \theta_{si} & |V_s| |V_i| \cos \theta_{si} \end{bmatrix} \quad (12)$$

The necessary and sufficient condition for voltage instability occurrence at bus i is singularity of the Jacobian matrix (J). Thus, the voltage stability boundary condition is that the determinant of the matrix J is equal to zero (i.e., $\det(J) = 0$). By solving the $\det(J) = 0$ equation, the voltage stability boundary condition at bus i is,

$$\frac{|V_i| \cos \theta_{si}}{|V_s|} = \operatorname{Re} \left[\frac{V_i}{V_s} \right] = \frac{1}{2} \quad (13)$$

With respect to (13), the ratio of voltages is equal to,

$$\frac{V_i}{V_s} = \frac{1}{2} + jc \quad (14)$$

where c is a real number.

Equation (6) can be rewritten as,

$$\frac{Z_{ii} S_i^*}{|V_i|^2} = 1 - \frac{V_s}{V_i} \quad (15)$$

Having (14) and (15), the following equation can be obtained equal to 1,

$$\left| \frac{Z_{ii} S_i^*}{|V_i|^2} \right| = \left| 1 - \frac{V_s}{V_i} \right| = \left| 1 - \frac{1}{\frac{1}{2} + jc} \right| = 1 \quad (16)$$

Equation (16) can also be written as,

$$r_i = \left| \frac{1}{Z_i S_i^*} \right| |V_i|^2 = \frac{|S_{AC,i}|}{|S_i^*|} = \frac{|V_i|^2}{|S_i^* Z_i|} = 1 \quad (17)$$

Equation (17) shows that the voltage instability at bus i takes place when the short-circuit capacity (i.e., $|S_{AC,i}|$) is smaller than the amount of inverter-based power generation at bus i . In other words, when the ratio r_i is smaller than 1, the voltage instability takes place at bus i , and when the ratio r_i is larger than or equal to 1, the voltage at bus i is stable.

3.1.2 Relation between static voltage stability and system strength

The strength of a power grid can be evaluated with the basic SCR measure, which is the ratio of the short circuit capacity at the point of interconnection of inverter-based generation unit to the rated capacity of the generation unit. When an inverter-based generation unit is connected to a power grid at bus i , SCR at bus i can be represented as (1). Comparing (1) and (17), we can see that SCR_i in (1) and r_i in (17) are the same when the injected power S_i in (17) is equal to the rated power of inverter-based generation unit $P_{DC,i}$. That is,

$$SCR_i = r_i = \frac{|S_{AC,i}|}{P_{DC,i}} = \frac{|V_i|^2}{P_{DC,i} |Z_i|} \quad (18)$$

Equation (18) represents that SCR_i quantifies the strength of the power grid at bus i in terms of the distance to voltage instability limit at bus i . Higher value of SCR_i means the system is stronger at bus i , since the voltage at bus i is more distant from its voltage

instability limit. When SCR_i is closer to 1, the power system at bus i becomes weaker, since the voltage at bus i is closer to its instability limit.

3.2 Site Dependent Short Circuit Ratio (SDSCR) for system strength evaluation

The inverter-based generation units interact with each other when they are electrically close to each other. The interactions affect the system strength at the points of interconnection; however, the effect of the interaction is not considered in the basic SCR measure defined in (18). In this section, a SCR-based measure will be defined to take into account the effect of the interactions on system strength evaluation by extending the relationship between basic SCR and voltage stability in a power grid with single inverter-based generation unit to a power grid with multiple inverter-based generation units. First, the voltage stability in a power grid interconnected to multiple inverter-based generation units is studied. Then, the SDSCR is proposed based on findings of the aforementioned study for system strength evaluation.

3.2.1 Study of voltage stability in a power grid with multiple inverter-based generation units

For the power grid interconnected to multiple inverter-based generation units shown in Figure 11, the network equation can be represented as,

$$\begin{bmatrix} \mathbf{V}_G \\ \mathbf{V}_R \end{bmatrix} = \begin{bmatrix} \mathbf{Z}_{GG} & \mathbf{Z}_{GR} \\ \mathbf{Z}_{RG} & \mathbf{Z}_{RR} \end{bmatrix} \begin{bmatrix} \mathbf{I}_G \\ \mathbf{I}_R \end{bmatrix} \quad (19)$$

where I_G and I_R are vectors representing the currents injected into the synchronous generator connected buses, and to inverter-based generation unit connected buses,

respectively; V_G and V_R are vectors representing voltages at the synchronous generator connected buses, and at the inverter-based generation unit connected buses, respectively; Z_{GG} , Z_{GR} , Z_{RR} and Z_{RR} are corresponding portions of the bus impedance matrix.

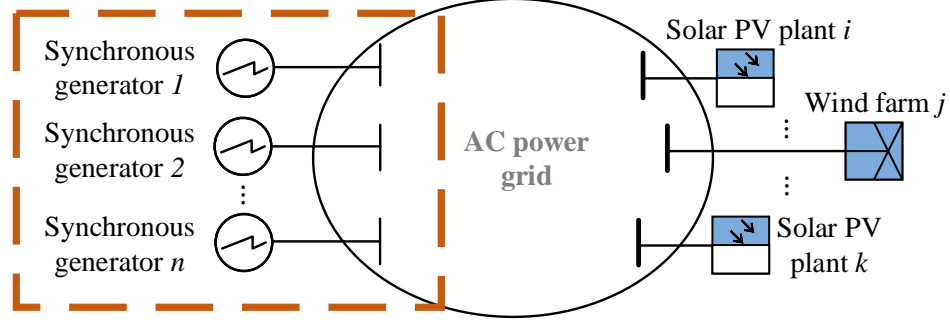


Figure 11. An AC power grid with multiple inverter-based generation units

Based on (19), the voltage stability boundary condition can be derived for the power gird shown in Figure 11. More specifically, with respect to (19), the voltage at point of interconnection i to which the inverter-based generation unit (i.e., solar PV plant i) is interconnected can be represented as,

$$V_{R,i} = \sum_{k \in G} Z_{RG,ik} I_{G,k} + Z_{RR,ii} \sum_{j \in R} \frac{Z_{RR,ij}}{Z_{RR,ii}} I_{R,j} \quad (20)$$

where $V_{R,i}$ is the i^{th} element in voltage vector \mathbf{V}_R ; $I_{G,k}$ and $I_{R,i}$ are the k^{th} element and i^{th} element in the current vectors \mathbf{I}_G and \mathbf{I}_R , respectively; $Z_{RG,ik}$ is the $(i, k)^{\text{th}}$ element in matrix \mathbf{Z}_{RG} ; $Z_{RR,ij}$ is the $(i, j)^{\text{th}}$ element in matrix \mathbf{Z}_{RR} ; \mathbf{G} is the set of all buses connected to synchronous generators, and \mathbf{R} is the set of all points of interconnection interconnected to the inverter-based generation units.

Equation (20) can be rewritten as,

$$\frac{V_{R,i} - V_{s,i}}{Z_{RR,ii}} = I_{eq,i} = \left(\frac{S_{eq,i}}{V_{R,i}} \right)^* \quad (21)$$

where,

$$V_{s,i} = \sum_{k \in G} Z_{RG,ik} I_{G,k} \quad (22)$$

$$I_{eq,i} = \sum_{j \in R} \frac{Z_{RR,ij}}{Z_{RR,ii}} I_{R,j} = I_{R,i} + \sum_{j \in R, j \neq i} \frac{Z_{RR,ij}}{Z_{RR,ii}} I_{R,j} \quad (23)$$

$$S_{eq,i} = V_{R,i} I_{eq,i}^* = V_{R,i} \left(I_{R,i}^* + \sum_{j \in R, j \neq i} \frac{Z_{RR,ij}^*}{Z_{RR,ii}^*} I_{R,j}^* \right) = \left(S_{R,i} + \sum_{j \in R, j \neq i} \frac{Z_{RR,ij}^*}{Z_{RR,ii}^*} \frac{V_{R,i}}{V_{R,j}} S_{R,j} \right) \quad (24)$$

Equation (21) is similar to (5), which is the network equation of a two-bus power grid. Similarly, (21) can be considered as the network equation of a two-bus power grid as shown in Figure 12, which is the equivalent model of the power grid in Figure 11 referred at bus i . In the equivalent system shown in Figure 12, $V_{s,i}$, $Z_{RR,ii}$, and $S_{eq,i}$ represent the voltage source, Thevenin impedance and the complex power injected into bus i in the equivalent two-bus power grid. As shown in (24), the equivalent injected power $S_{eq,i}$ includes the power injected from the inverter-based generation unit interconnected to point of interconnection i (i.e., $S_{R,i}$), and the power injected from other inverter-based generation units (i.e., $S_{R,j}$).

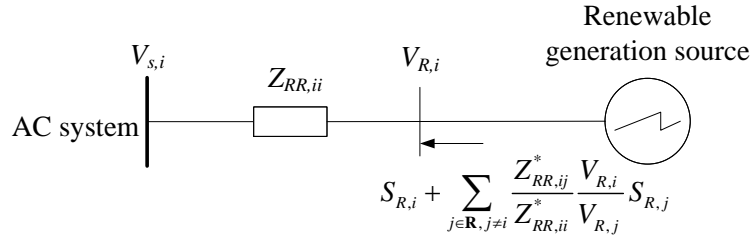


Figure 12. Equivalence of an AC power grid with multiple inverter-based generation units

In line with the derivation shown in (7)-(13), equation (14) can be utilized to derive the voltage stability boundary condition for the voltage at bus i in the power grid interconnected to multiple inverter-based generation units as follows,

$$\frac{|V_{R,i}| \cos \theta_{si}}{|V_{s,i}|} = \operatorname{Re} \left[\frac{V_{R,i}}{V_{s,i}} \right] = \frac{1}{2} \quad (25)$$

By plugging (25) into (21), the voltage stability boundary condition in (25) can be rewritten as,

$$\bar{r}_i = \frac{|S_{ac,i}|}{|S_{eq,i}^*|} = \frac{|V_{R,i}|^2}{|S_{eq,i}^* Z_{RR,ii}|} = \frac{|V_{R,i}|^2}{|(P_{eq,i} - jQ_{eq,i}) \| Z_{RR,ii}|} = 1 \quad (26)$$

where,

$$P_{eq,i} = P_{R,i} + \sum_{j \in R, j \neq i} (P_{R,j} w_{ij} \cos \alpha_{ij} - Q_{R,j} w_{ij} \sin \alpha_{ij}) \quad (27)$$

$$Q_{eq,i} = Q_{R,i} + \sum_{j \in R, j \neq i} (P_{R,j} w_{ij} \sin \alpha_{ij} + Q_{R,j} w_{ij} \cos \alpha_{ij}) \quad (28)$$

$$w_{ij} = \frac{|Z_{RR,ij}| |V_{R,i}|}{|Z_{RR,ii}| |V_{R,j}|} \quad (29)$$

$$\alpha_{ij} = \theta_{RR,ii} - \theta_{RR,ij} + \delta_{R,i} - \delta_{R,j} \quad (30)$$

where $P_{eq,i}$ and $Q_{eq,i}$ are the real and imaginary parts of the complex power $S_{eq,i}$ in (24); $\theta_{R,ij}$ is the angle of impedance $Z_{RR,ij}$; and $\delta_{R,i}$ is the angle of bus voltage $V_{R,i}$.

Equation (26) shows that when the ratio \bar{r}_i is larger than or equal to 1, the voltage at bus i is stable, and when the ratio \bar{r}_i is equal to 1, the voltage instability happens at bus i .

3.2.2 SDSCR measure and features

Equations (26)-(30) are the basis for the SDSCR measure that can be used to evaluate the system strength at each point of interconnection in terms of proximity to voltage instability limit. As shown in (1), the basic SCR measure evaluates the system strength with a single inverter-based generation unit in terms of the distance to voltage stability limit. Similarly, in a power grid with multiple inverter-based generation units, a new SCR-based measure can be defined based on (26) to evaluate the system strength at point of interconnection i in terms of the distance to voltage stability limit as follows,

$$SDSCR_i = \frac{|V_i|^2}{P_i + \sum_{j \in R, j \neq i} P_j w_{ij} \cos \alpha_{ij} |Z_{RR,ii}|} \quad (31)$$

Chapter 4: Particular Features and Applications of SDSCR Measure

In this chapter, privileges of the proposed SDSCR measure over the existing SCR-based measures are discussed and illustrated using a test power system. In addition, applications of this measure in power grid structural analysis and integration studies of renewable energy resources are presented. It is also discussed that evaluation of system strength at the points of interconnection of renewable energy resources can be even more precise by more accurate forecast of renewable power generation based on knowledge of weather condition.

4.1 Particular privileges of SDSCR over existing methods

The SDSCR measure shown in (31) has some particular features, which make it an enhanced measure for system strength evaluation over the existing ones. The features are included but not limited to the following items,

- The SDSCR measure is the general representation of the basic SCR shown in (1). Comparing the basic SCR in (1) with SDSCR in (13) implies that the basic SCR is a special case of the SDSCR where only one inverter-based generation unit is interconnected to the power grid. In other words, the SDSCR is the same as the basic SCR with P_j equal to zero for all others inverter-based generation units. When multiple inverter-based generation units are interconnected to a power grid, but they are electrically very far from each other, the electrical distance ($Z_{RR,ij}$) between any pair of the inverter-based generation units is very small and the ratio

of electrical distance (i.e., $Z_{RR,ij}/Z_{RR,ii}$) is close to zero. Thus, the SDSCR is approximately equal to the basic SCR.

SDSCR is a general representation of the basic SCR, which can be used to evaluate the strength in a power grid interconnected to either single inverter-based generation unit or multiple ones.

- The SDSCR can evaluate the system strength in terms of the distance to voltage stability limits,

Equation (31) shows that SDSCR is defined based on the voltage stability boundary condition derived in (26); hence it evaluates the system strength in terms of the distance to voltage stability limits. When the value of SDSCR at bus i is bigger than 1, the voltage at point of interconnection i is stable, since it is distant from its instability limit. When the value of SDSCR at bus i is close to 1, it implies that the point of interconnection i is weak and there is risk of voltage instability occurrence, since the voltage is close to its stability limit.

- It provides the information on the system strength at each particular point of interconnection,

The SDSCR evaluates the system strength with respect to each point of interconnection of inverter-based generation unit. When multiple inverter-based generation units are electrically close in a common area, the SDSCR can be used to identify the weakest/strongest point of interconnection in the area for the system strength improvement/integration of new units.

- It uses power grid structural-related factors⁴ to take the interactions among the inverter-based generation units into account of system strength evaluation,

In (31) the SDSCR measure at bus i takes into account not only the power injected from the inverter-based generation unit at point of interconnection i (i.e., P_i), but also the power injected from other inverter-based generation units interconnected to other points of interconnection in the power grid (i.e., P_j).

Specifically, the power P_j is scaled by the weight shown in (29). This weight shows that the effect of other inverter-based generation units on the system strength at point of interconnection i depends on the ratio of electrical distance $Z_{RR,ij}/Z_{RR,ii}$ and the ratio of bus voltages $V_{R,i}^*/V_{R,j}^*$. The inverter-based generation unit interconnected to point of interconnection j significantly affects the system strength at point of interconnection i when the electrical distance between inverter-based generation unit j and point of interconnection i (i.e., $Z_{RR,ij}$) is close to Thevenin impedance at bus i (i.e., $Z_{RR,ii}$), and the voltage at bus i is close to the one at bus j . Thus, when multiple inverter-based generation units are electrically close to each other in a common area with similar bus voltages, their interactions significantly affect the system strength at each other's points of interconnection.

⁴ In power system engineering, structural-related factors are parameters that are only based on the power grid structural characteristics (electrical connectivity) and remain constant when operating condition varies. For example, Generation Shift Factor (GSF), Power Transfer Distribution Factor (PTDF), elements of power grid impedance matrix (Z_{bus}) are all structural-related factors.

4.2 Power grid structural analysis using SDSCR

The SDSCR measure introduced in (31) evaluates the system strength based on the power grid structural-related factors. More specifically, in evaluating the system strength at point of interconnection i , this measure takes into account the impact of other inverter-based generation units (P_j) on the system strength at point i through scaling their impacts by a weight (w_{ij}) in which characteristics of the power grid structure and voltage stability are considered. This feature defines another useful application for this measure, which is power grid structural analysis.

To illustrate it, consider the SDSCR equation in (31) and let $V_{R,i}$ and $V_{R,j}$ be equal to $1.0\angle 0^\circ$ per unit. Then, (31) can be approximately represented as,

$$SDSCR_i = \frac{1}{P_i + \sum_{j \in \mathbf{R}, j \neq i} P_j \times \Delta} \quad (32)$$

where,

$$\Delta = \left(\frac{|Z_{RR,ij}|}{|Z_{RR,ii}|} \cos(\theta_{RR,ii} - \theta_{RR,ij}) |Z_{RR,ii}| \right) \quad (33)$$

Equation (33) further explains the impact of the interactions among multiple inverter-based generation units on the system strength of the AC power grid at point of interconnection i from the structural perspective. As shown in (32), the power injected into bus i from the other inverter-based generation units is scaled by Δ in (33), which is a completely structural-related factor. Basically Δ is comprised of the ratio of two electrical distances $Z_{RR,ij}$ and $Z_{RR,ii}$. That are,

- $Z_{RR,ii}$ is the electrical distance between the inverter-based generation unit of interest interconnected to point of interconnection i and the AC power grid (i.e., the Thevenin equivalence impedance at bus i).
- $Z_{RR,ij}$ is the electrical distance between the inverter-based generation unit at the point of interconnection j and the AC power grid seen from point of interconnection i .

Based on the ratio of electrical distances, it can be seen that the inverter-based generation unit interconnected to point j has a significant impact on system strength at point of interconnection i if the electrical distance between generation unit j and point i (i.e., $Z_{RR,ij}$) is close to the Thevenin impedance at point i (i.e., $Z_{RR,ii}$). When multiple inverter-based generation units are electrically close to each other in a common area, their electrical distances $Z_{RR,ij}$ are close to $Z_{RR,ii}$; and the interactions among them significantly affect the system strength of the AC power grid at point of interconnection i .

Hence an AC power system with multiple generation sources as shown in Figure 11 can be represented with an equivalent system as shown Figure 12. In the equivalent system, an equivalent inverter-based generation unit is connected to the AC power grid via a transmission line with impedance $Z_{RR,ii}$. The total inverter-based power injected into point i is equal to the power injected from generation unit at point i and other amounts of power injected from other plants, which are scaled by the ration of electrical distance (i.e, $P_i + \sum_{j \in \mathbf{R}, j \neq i} P_j \times \Delta$).

This property of SDSCR is very useful in power grid structural analysis, identifying the weak points of transmission/distribution system that should be strengthening and spotting the strong points of interconnection for future integration of renewable energy resources.

4.3 System strength evaluation for integration of renewable energy resources

Renewable energy resources are fast acting solid-state systems in which variations of generation can be dramatic, similar to sudden changes of load, such as failures or faults. In addition, they are usually interconnected to the locations where, transmission or distribution system is weak from the power grid structure perspective, and less sophisticated voltage support is provided to the points of interconnection. All these concerns make the system operators to study the impact of renewable energy resources on the power grid operating condition and stability status, specifically, voltage stability and VAR sufficiency.

From voltage stability perspective, performance of various components in a power grid is highly dependent on the system strength. Hence system strength is a common concern in the integration of renewable energy sources. Voltage stability issues may be caused by high penetration of renewable energy resources into a weak grid. The renewable connected areas have some specific characteristics including,

- Delivering renewable power from remote areas to load zones through long EHV transmission lines,

- Locating at remote regions, far away from synchronous generators and load zones with sophisticated voltage support equipment,
- Integrated by means of significant power electronic devices to provide system support.

These characteristics commonly makes the power grid weak at the points of interconnection of renewable energy resources, such as wind farms and utility-scale solar PV plants. In a weak power grid,

- SCR is low at the points of renewable energy resources,
- voltage is not stiff at the points of interconnection and there are several challenges for voltage control,
- maintaining the quality of load service (i.e., power grid performance and voltage stability) is dominated by,
 - the system operating condition, such as summer peak or spring off-peak, and,
 - variations in the weather condition, such as high wind, low wind and rate of solar irradiance, etc.

The basic SCR is commonly used as a measure for the system strength evaluation. This calculation method does not consider the interactions among the renewable energy resources, therefore gives an optimistic estimation of the system strength. To overcome this issue, two SCR-based measures have been developed by ERCOT and GE, which are being used by the power industry to calculate the SCR for the purpose of system strength

evaluation. These measures have some limitations that may result in imprecise evaluation of system strength. For example, they are unable to evaluate the system strength at each specific point of interconnection.

The proposed SDSCR measure can be used as an enhanced method of system strength calculation over the existing ones used by GE and ERCOT. Compared to the basic SCR, WSCR by ERCOT, and CSCR by GE, the SDSCR measure has some privileges as follows, (a) it evaluates the system strength in terms of the distance to static voltage stability limit, (b) it takes the effect of interaction among renewable generation sources into account of calculations, and (c) it provides information on the system strength at each specific point of interconnection.

4.4 Implementation and validation of SDSCR measure

4.4.1 Approach of validation study

The validity of the system strength evaluation results obtained from the four measures (i.e., basic SCR, WSCR, CSCR and SDSCR) is investigated and compared through the following major steps:

- Performing P-V analysis for the point of interconnection of interest,
- Setting up the desired (critical) operating condition in the test power system,
- Evaluating the system strength at the point of interconnection using the four measures,
- Investigating validity of the results obtained from each measure using their thresholds and the set-up system operating condition,
- Summarizing the validation studies for various operating conditions.

Figure 13 shows a flowchart in which the detailed procedure and all the steps of the validation study are presented.

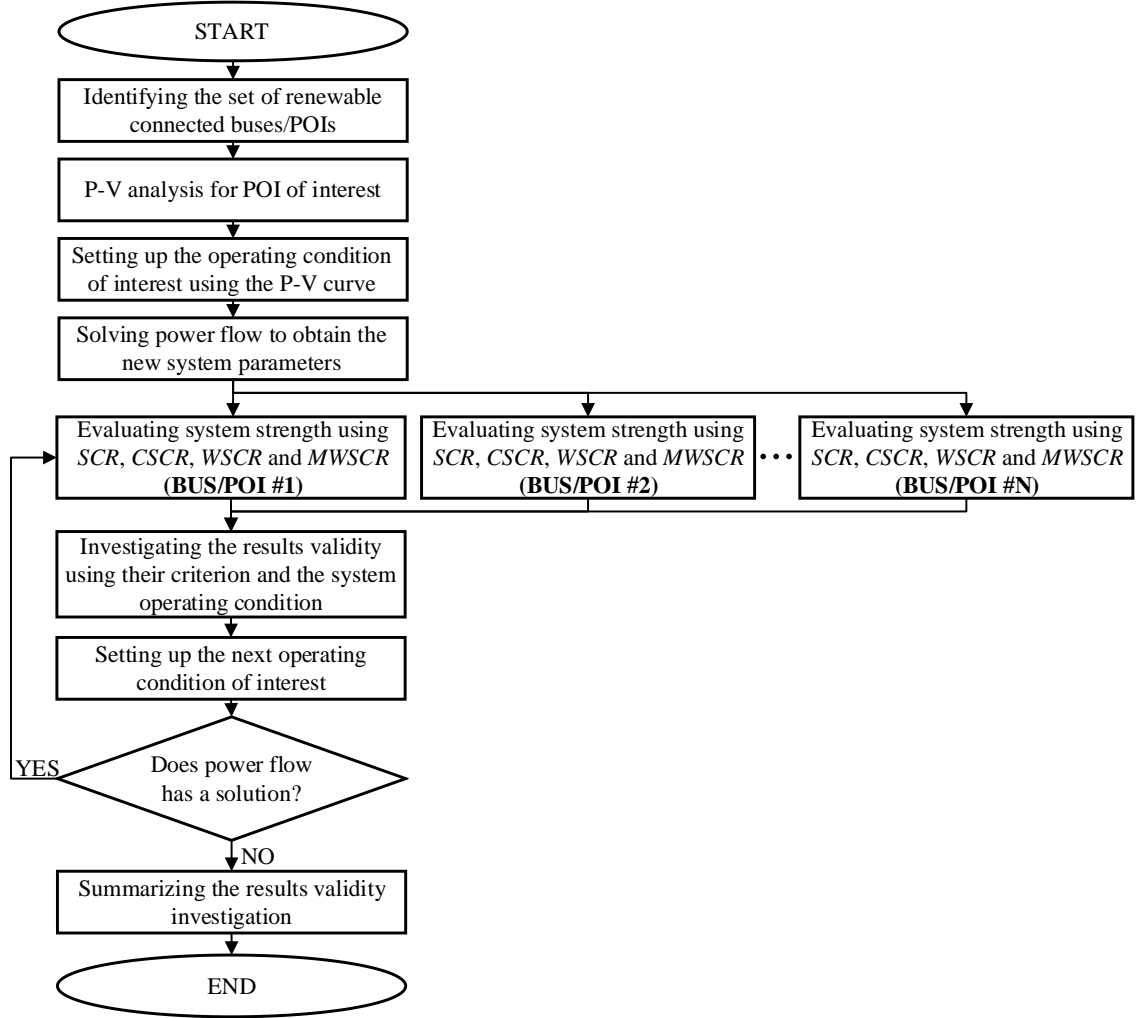


Figure 13. Flowchart of validation study

In this study, the P-V curve associated with the point of interconnection of interest is utilized to obtain and set-up particular operating conditions in studying power system. The P-V (Active Power-Voltage) curve calculation involves using a series of power flow solutions for increasing injection/transfer of power and monitoring the associated impacts on the voltage profile of the load and transfer buses. More specifically, it is a steady-state

tool that develops a curve, which relates the voltage at each bus to variations of power generation/load level within an area. As shown in Figure 14, each P-V curve is comprised of the three following particular points,

A. Nose point (also called critical point),

At this point (i.e., point C) voltage drops rapidly with an increase in MW transfer. For power injection beyond this point power flow solution fails to converge, which represents voltage instability.

B. Near the critical operating point,

Operating the power grid in a close neighborhood of this point (i.e., point B) involves high risk of voltage stability issues, such as a large-scale blackout. Under this operating condition, with a small increase of power injection the system may enter into the unstable area

C. Reliable operating point/zone,

Operating the power grid at this point (i.e., point A, and curve segment between points A and B) ensures the voltage stability at the bus of interest.

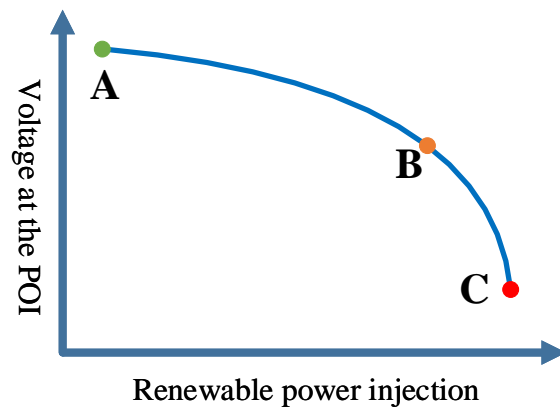


Figure 14. P-V curve with important points

Calculating the P-V curve includes increasing the renewable capacity in specific steps sizes, solving power flow for the new renewable capacity, recording and plotting the associated voltage at the point of interconnection for each new renewable capacity.

The P-V curve is used to set up a particular case study; then the threshold of each measure is used for evaluating the system strength. The result obtained from each measure is valid if the evaluated system strength is consistent with the set-up (i.e., actual) operating condition of the system.

4.4.2 Validation study using WSCC 9-bus system

In order to illustrate the accuracy of system strength evaluation for integration of renewable energy resources using SDSCR measure, and demonstrate its privileges over the existing measures, the validity of the system strength evaluation results obtained from each measure (i.e., basic SCR, WSCR, CSCR and SDSCR) are investigated under a critical operating condition. To this end the WSCC 9-bus system is used as shown in Figure 15. In this system, a 60 MW and a 100 MW solar PV plants are interconnected to points of interconnection/buses 3 and 8, and the system strength is evaluated at these two locations under a critical operating condition.

To set up a critical operating condition, the P-V curve associated with bus 3 is calculated as shown in Figure 16. The P-V curve is used to find the amount of renewable power generation for which voltage instability happens at bus 3 (i.e., power flow does not converge). This operating condition can be obtained from the “nose point” of the P-V curve, which is 107MW renewable power generation at bus 3. Increase of even 1MW

renewable power generation at bus 3 will lead to voltage collapse. Under this operating condition, the system strength is evaluated at buses 3 and 8 using the four measures.

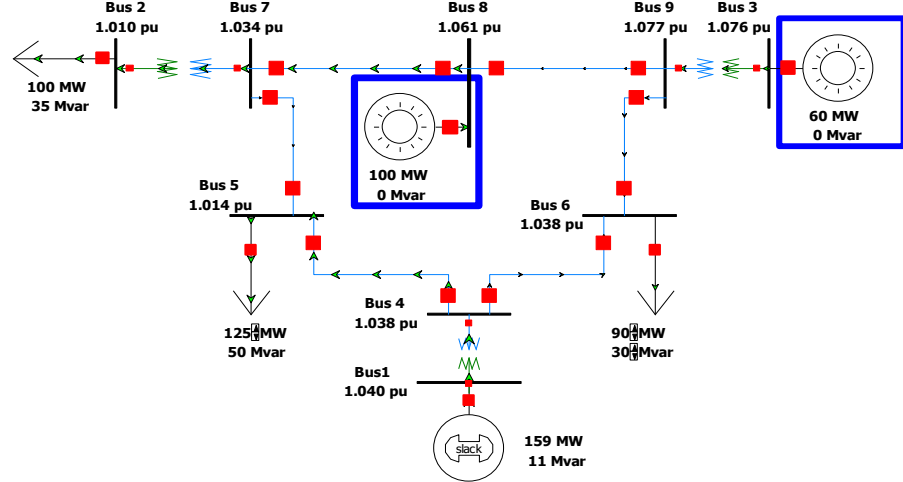


Figure 15. WSCC 9-bus system with two renewable energy resources

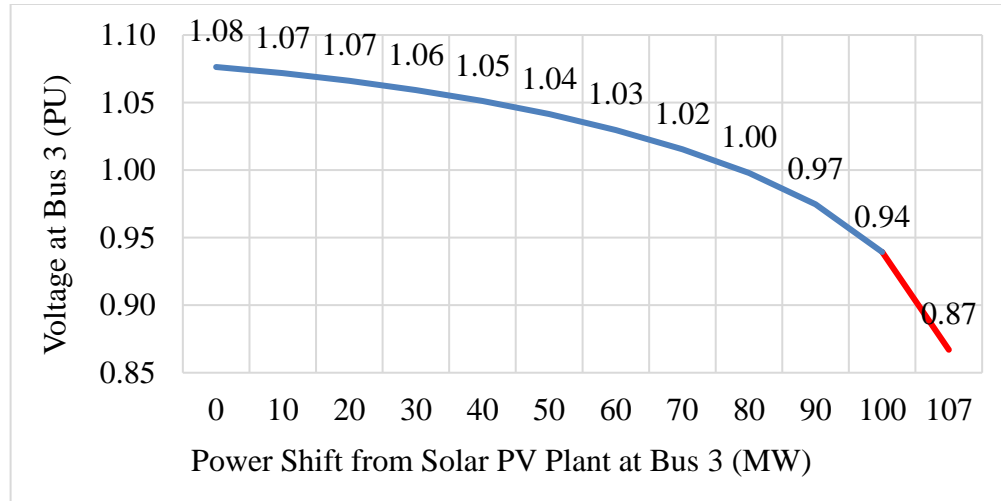


Figure 16. P-V curve at bus 3

Table 1 shows the results of the system strength evaluation study using the four methods at the renewable energy resource interconnected buses 3 and 8.

Table 1. System strength evaluation results (WSCC 9-bus system)

Bus#	Measure	Calculated SCR	Expected SCR	Results Validity
Bus #3 (POI ⁵ of interest)	Basic SCR	2.7319	1	overestimated
	CSCR	1.2856	smaller than 1	overestimated
	WSCR	1.6015	smaller than 1.5	overestimated
	SDSCR	1.0054	1	valid
Bus #8 (Renewable connected)	Basic SCR	2.0071	smaller than 2	overestimated
	CSCR	1.2856	smaller than 1	overestimated
	WSCR	1.6015	smaller than 1.5	overestimated
	SDSCR	1.2509	close to 1	valid

In Table 1, the 2nd column shows what measure is used to evaluate the system strength at buses 3 and 8; the 3rd column represents the value of SCR calculated using the measure in the corresponding row; the 4th column shows the expected value of the SCR for this specific critical operating condition, which is very close to voltage instability occurrence; the 5th column shows if the results of the system strength evaluation obtained from each measure is match with the expected value.

As it can be seen, the basic SCR, CSCR and WSCR measures overestimated the system strength, particularly at the point of interconnection/bus 3. The basic SCR overestimates the system strength at the both points of interconnection, since it does not consider the (interaction) impact of renewable power generation at the other point of interconnection on the studied point. In addition, the CSCR and WSCR measures provide identical results for the both points of interconnection, which is not the case as shown by the basic SCR and SDSCR measures.

The results obtained from the SDSCR show that the power grid is operating at the voltage instability limit at the point of interconnection/bus 3. It is able to provide

⁵ POI: Point of interconnection of a renewable energy resource.

particular system strength evaluation result for each point of interconnection, which implies the power grid is very weak at point of interconnection/bus 8. The results of system strength evaluation based on the SDSCR measure are reasonably match with the set-up operating condition of the system.

4.5 Improved system strength evaluation based on more accurate forecast of renewable power generation

Currently utility-scale wind farms and solar PV plants are two major renewable energy resources that are taking over a significant portion of power generation in modern power grids. The proposed SCR-based measure (SDSCR) can be utilized to evaluate the system strength at their points of interconnection in terms of voltage stability. In using all SCR-based measures, traditionally the full-capacity of renewable energy resources are used for calculating the SCR. That is, calculating the bus voltages (i.e., V_i, V_j) when renewable energy resources are generating at their full-capacity, and using the amounts of renewable power generations (i.e., P_i, P_j) at the points of interconnection equal to their full-capacity.

In real-world operation, variations of weather condition significantly affect the amount of power generation by the wind farms and solar PV plants. Using accurately estimated amounts of renewable power generation (i.e., renewable energy resources operating condition) instead of full-capacities will provide more realistic system strength evaluation results. To illustrate it, let's consider evaluating the system strength using the SDSCR measure introduced in (31). In this equation, P_i and P_j would be traditionally equal to the full-capacity of the wind farms and/or solar PV plants. However, in real-

world these quantities are often not equal to their full-capacities due to the variations of weather condition, such as sudden drops of solar irradiance, change of clouds distribution over solar PV plants, variations of wind speed in wind farm locations, etc. Hence more realistic estimation of renewable power generations would be P_i^* and P_j^* , which can be obtained based on variations of weather condition. Similarly, V_i and V_j would be the functions of P_i^* and P_j^* , that are the estimated amount of renewable power generations at the points of interconnection i and j . Using the realistic values of renewable power generation and bus voltages (i.e., P_i^* , P_j^* , V_i^* and V_j^*) estimated based on weather condition data, (31) can be re-written as follows,

$$SDSCR_i = \frac{|V_i^*|^2}{P_i^* + \sum_{j \in R, j \neq i} P_j^* \left(\frac{|Z_{RR,ij}| |V_{R,i}^*|}{|Z_{RR,ii}| |V_{R,j}^*|} \right) \cos \alpha_{ij} |Z_{RR,ii}|} \quad (34)$$

Evaluating the system strength based on (34) will provide more informative and realistic results. Using (34) requires accurate estimation of wind farms and solar PV plants power generation. Hence in this research: (a) a SAS-based algorithm is proposed for estimation of actual power curve (i.e., power generation of a wind farm vs. wind speed) of a wind farm, and (b) a method is developed for estimation of solar power generation based on distribution of clouds over the solar PV plants.

4.5.1 Estimation of wind farms power generation

An accurate estimation of power curves is essential for assessing the actual output characteristics of a wind farm, as the power curve provided by the manufacturer changes after several years of operation. The power curve can be estimated using the measured

power output data comprising wind power generation and wind speed. However, these measured data are generally ill-distributed due to significant number of outliers, which impose a serious bias challenging estimation of power curves. In this research, an intelligent algorithm is proposed for estimating power curves using the measured data while minimizing modeling and bias errors caused by outliers in the data. Particularly, the proposed algorithm is designed based on Statistical Analysis Software (SAS) package in order to facilitate the analysis of a big dataset.

4.5.2 Estimation of solar PV plants power generation

The amount of solar power generation is significantly dependent on the weather and atmospheric conditions. In this research, a method is developed to forecast the amount of solar power generation based on information of clouds distribution. To obtain the clouds distribution, the time-series weather data is used to train an Artificial Neural Network (ANN) model that forecasts the solar irradiance. The model's associated forecast errors are considered as a measure to define several cloud modes which can be used to estimate the realistic solar PV plant operating condition including the amount and sudden drops of solar power generation.

Chapter 5: A SAS-based Algorithm for Estimation of Actual Power

Curve of a Wind Farm/Turbine Based on Operation Data

5.1 Introduction to wind power curve estimation

Significant penetration of wind energy into modern power systems raises concerns regarding uncertainties in the power generation of wind farms. The uncertainties included in wind power generation and variations of generation pattern may result in serious reliability and/or operational problems, such as reactive power margin issues at the point of interconnection of wind farms to the power grid or creation of simultaneously congested lines where generation zones meet load zones, [21], [22]. Hence several studies have been carried out to investigate the impact of the increased penetration of renewable sources including wind energy on the overall reliability and stability of the power system, [23]–[29]. In the studies, it is essential to provide the accurate estimation of the wind turbine power curve, [30]. This curve displays the generation pattern of a wind turbine for different wind speed levels. As shown Figure 17, a typical wind turbine power curve has three critical points:

- A. Cut-in speed (S_{in}): for this wind speed, the wind turbine starts generating power. This point is also known as the wind turbine generation threshold.
- B. Rated speed (S_r): for this wind speed, power generation reaches the rated generation capacity of the wind turbine.
- C. Cut-out speed (S_o): at this point, the wind turbine stops generating to prevent possible hardware damages. An accurate power curve would be beneficial for

system planning purposes, wind farm efficiency assessment, wind turbine fatigue analysis and power market analysis.

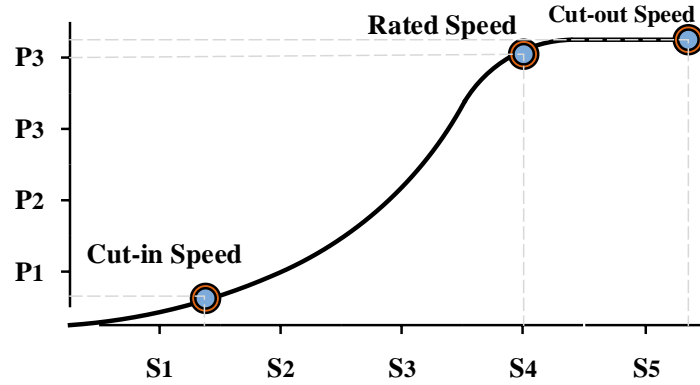


Figure 17. A typical wind turbine power curve with the critical points

Estimating an accurate power curve that can be used in real-world operations is a challenge for wind farm owners or power system operators. A wind turbine manufacturer provides a theoretical power curve of its wind turbine for planning purposes and estimating total wind power production. However, the power curve observed by the operator in practice can be substantially different due to several factors, such as wind farm location, meteorological conditions, turbine fatigue, and errors included in wind forecast and/or generation output measurements, etc., [31]. In the literature, different techniques are developed to estimate power curves using historical data. In [30] a data-mining based approach is developed for power curve monitoring. For this purpose, cluster center fuzzy logic, neural network, and k-nearest neighbor models are built and their performances are compared against others in the literature. In [31] the research investigates how to obtain an equivalent power curve model of a wind farm using field measurement data for individual wind turbines at the site. In [32] the differential evolution algorithm is applied to a five-parameter logistic function to determine a parametric model

for a power curve. In [33] calibration of the power curve is studied by building a fitted regression model. In [34] a power curve monitoring method is developed, which may prevent a wind turbine failure. The method finds the power curve limits for the purpose of power curve monitoring. In [35] the research presents a comparative analysis of various parametric and non-parametric techniques for modeling the power curves. In [36] a study of on-line power curve monitoring is presented. The study is performed through developing power curve models using least squares and maximum likelihood estimation methods. In [37] a power curve model is developed based on the Gaussian process by using the maximum likelihood optimized approach to find the optimal hyper-parameters. In [38] a controller curve introduced to develop a method for modifying the power curve with respect to wind dynamics. In [39] normalized power curves are proposed to develop a method for matching wind turbines to a site using the normalized curves. In [40] a probabilistic model is proposed to characterize the dynamics of the wind turbine power output to develop dynamic power curves. In [41] parametric and nonparametric methods are used to estimate the wind turbine power curve by a locally weighted polynomial regression method. In [42] the power curve characteristics are used to model the power curve by cluster center, fuzzy c-means clustering, subtractive clustering and polynomial methods. In [43] nested Markov chain approach is used for statistical representation of the equivalent power curve. In [44] the operational data from wind turbines are utilized to estimate bivariate probability distribution functions that represent the power curve. To this end, statistical application of empirical copulas is used to estimate the power curve such that operational deviations from the expected behavior can be detected. In [45] it is shown that the joint probability distribution of wind power generation and wind speed

can be obtained from data, rather than from examination of the implied function of the two variables. Based on this property, they developed a model that can be used to simulate the plant behavior.

In the previous works, it is still a challenge to estimate an accurate power curve that can be used in real-world operation. The existing techniques pay less attention to reducing the bias imposed to the estimated model by several outliers in an actual dataset; thus, zero observations usually occur in the wind power generation-wind speed dataset as shown in Figure 18. These outliers impose noticeable impacts on the estimated power curve; thus, it is very important to appropriately clean the outliers out in the dataset for estimating an accurate power curve such that the bias and modeling error are simultaneously minimized. In addition, the existing techniques predict the power curve based on fixed frameworks that may just work fine for some particular datasets. In other words, they are not designed with the flexibility to update their prediction approaches with respect to the unique characteristics of each particular dataset. The importance and practical usefulness of estimating an accurate and close to real-world power curve motivates us to address the challenge of estimating an accurate power curve directly from real-world data with minimized bias and modeling errors for wind turbine/wind farm operation assessment purposes.

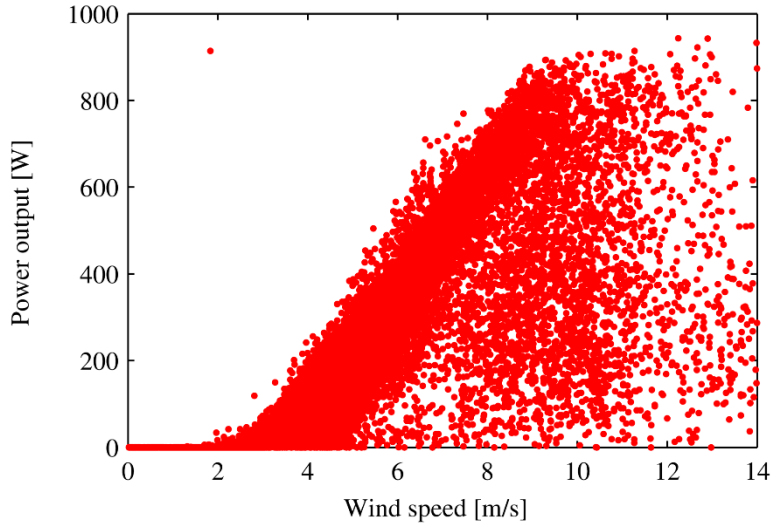


Figure 18. A wind turbine power generation-wind speed raw data

In this chapter, a SAS-based algorithm is proposed to estimate power curves using the real dataset of wind power generation and wind speed while simultaneously minimizing both the modeling and bias errors. SAS (Statistical Analysis System) is a software package for advanced analytics, multivariate analyses, data management and predictive analytics. Compared with these programming packages SAS has several powerful and specific features which are specifically designed for statistical and data analyses, [46]. Some of the major features can be summarized as follows,

- SAS is comprised of comprehensive collections of basic to advanced statistical modules (i.e., Procedures) for processing, mining and analyzing data. These modules are very useful for efficient analysis of big datasets, such as wind power generation-wind speed time-series datasets.

- Unlike many other statistical packages, SAS is also an extremely powerful, general-purpose programming language. This feature significantly facilitates the automation of the recursive simulations required by the proposed algorithm.
- SAS is not commonly used in power industry. Development of a SAS-based algorithm that accurately estimates the average wind turbine power curve can introduce a powerful data analysis tool to power engineers who are interested in analyzing big datasets.

In the algorithm, a continuously updated piece-wise linear model is used to minimize modeling errors while bias errors are reduced by using SAS package to recursively clean outliers out in the real dataset of wind power generation and wind speed. As a result of being SAS-based, the algorithm is designed to be self-adaptive, which makes it applicable to a variety of datasets including any kind of bias or undesirable observations. Before we introduce the algorithm, first the theoretical foundation of creating a data-driven power curve model is provided, and the modeling and bias errors caused by outliers in the measured dataset of wind power generation and wind speed are analyzed. Then, the algorithm is presented. The algorithm involves several recursive iterations, and at each iteration two major tasks are completed: (1) fitting a piece-wise linear model to the time-series wind power generation-wind speed data trend, and (2) cleaning data recursively using the piece-wise linear model as a benchmark. Task (1) is carried out through non-linear parameter estimation taking the data bias into consideration of modeling. Task (2) includes minimizing/eliminating the bias and modeling errors until the convergence criterion is met.

4.2 Model for estimation of power curves and error reduction

4.2.1 Data-Driven Model for Estimation of Power Curves

In order to formulate the estimated power curve model, let G denote the discrete-time wind power generation-wind speed dataset. This type of data is commonly collected at constant 5 or 10 minute intervals/increments,

$$G = \{(s_{(t)}, p_{(t)}) \mid t = 1, \dots, N\} \quad (35)$$

Equation (35) shows that dataset G includes the information of wind speed and wind turbine power generation at time t . The relation between the corresponded data points in (35) including the total error (i.e., the summation of errors involved in the estimated model) can be written in the following system estimation form, which is discussed in detail in [47],

$$p_{(t)} + \alpha_1 p_{(t-1)} + \dots + \alpha_{n_\alpha} p_{(t-n_\alpha)} = \beta_1 s_{(t-1)} + \dots + \beta_{n_\beta} s_{(t-n_\beta)} + e_{(t)} + \gamma_1 e_{(t-1)} + \dots + \gamma_{n_\gamma} e_{(t-n_\gamma)} \quad (t = 1, 2, \dots, N) \quad (36)$$

The expression in (36) can be used to estimate future wind turbine power generation, given the historical data (G) or an accurate wind speed forecast. Thus, the model output (wind turbine power generation) at time t including the total error can be written in the following form; however, the parameters in ξ are unknown,

$$\overline{\overline{p}}_{(t|\xi)} = \varphi_{(t)}^T \xi \quad (37)$$

At this stage, the objective is to identify the unknown parameters (i.e., ξ) such that the total error of the model becomes minimized. Using the least square technique,

the total error of model (37) can be defined equal to the average of sum of squares of total errors. The total least square error of the model is shown in (38),

$$E_N(\xi, G) = \frac{1}{N} \sum_{t=1}^N (\mathbf{p}_{(t)} - \overline{\overline{\mathbf{p}}}_{(t|\xi)})^2 \quad (38)$$

To find the unknown model parameters included in ξ , the following optimization problem should be solved over all ξ ,

$$\xi = \arg_{\xi} \min (E_N(\xi, G)) \quad (39)$$

where,

$$\frac{d}{d\xi} E_N(\xi, G) = 0 \quad (40)$$

Given the optimality condition in (40), and assuming that $\varphi_{(t)} \varphi_{(t)}^T \in R^{(n_\alpha + n_\beta + n_\gamma) \times (n_\alpha + n_\beta + n_\gamma)}$ is non-singular, the vector of estimated parameters is equal to,

$$\xi_N = (\varphi_{(t)} \varphi_{(t)}^T)^{-1} \varphi_{(t)} P_{(t)} \quad (41)$$

4.2.2 Errors Involved in Estimated Model

Dataset (G) includes a high-variance high-bias distribution. Hence careful investigation of errors that may be involved in the model is an essential part of developing an accurate estimated model. To analyze the errors involved in the estimated model, (38) can be represented with bias, modeling error and irreducible error components [42]. Specifically, we have:

$$E_N(\xi, G) = \psi_e^2 + \varepsilon_M^2 + B_e \quad (42)$$

where,

$$\varepsilon_M^2 = E[(\overline{\overline{\mathbf{p}}}_{(t|\xi)} - E[\overline{\overline{\mathbf{p}}}_{(t|\xi)}])^2] \quad (43)$$

$$B_e = (E[\overline{\overline{p}}_{(t|\xi)}] - \overline{p}_{(t|\xi)})^2 \quad (44)$$

In (42), ψ_e^2 , ε_M^2 and B_e represent the irreducible error, modeling error, and bias error. Each of these errors are briefly introduced and discussed below.

1) *Irreducible Error (ψ_e^2)*

The irreducible error is defined as a noise that exists in the real-world association between the wind power generation and the wind speed measurements. This error cannot be reduced by any of the modeling techniques; since we have no evident information available regarding its quality or quantity, and the reason that results in this type of error.

2) *Modeling Error (ε_M^2)*

With respect to (40), modeling error (i.e., variance) is the expected value of the difference between the model output and the expected output of the model (i.e., a perfect model). Reducing the modeling error of an estimated model (estimator) would noticeably improve the estimation precision.

The scientific basis behind the approach by which we improve the modeling error/variance of the model can be described using the following property of the conditional probability.

Property: The modeling error of an estimated model (i.e., an estimator) can be improved by introducing a condition on that estimator. That is,

$$Var(E[\overline{\overline{p}}_{(t|\xi)} | \kappa]) \leq Var(\overline{\overline{p}}_{(t|\xi)}) \quad (45)$$

where κ is defined as the minimum least square error.

Proof: Based on this property, variance of the model can be improved by setting a given condition on that. Let variance of the model be as follows,

$$E[\overline{\overline{p_{(t|\xi)}}} | \kappa] = E[E[\overline{\overline{p_{(t|\xi)}}}^2 | \kappa] - (E[\overline{\overline{p_{(t|\xi)}}} | \kappa])^2] \quad (46)$$

$$= E[E[\overline{\overline{p_{(t|\xi)}}}^2 | \kappa] - E[E[\overline{\overline{p_{(t|\xi)}}} | \kappa]^2] + (E[E[\overline{\overline{p_{(t|\xi)}}} | \kappa]])^2 - (E[E[\overline{\overline{p_{(t|\xi)}}} | \kappa]])^2] \quad (47)$$

$$= E[E[\overline{\overline{p_{(t|\xi)}}}^2 | \kappa] - Var[E[\overline{\overline{p_{(t|\xi)}}} | \kappa]] - (E[E[\overline{\overline{p_{(t|\xi)}}} | \kappa]])^2] \quad (48)$$

$$= E[\overline{\overline{p_{(t|\xi)}}}^2] - Var[E[\overline{\overline{p_{(t|\xi)}}} | \kappa]] - (E[\overline{\overline{p_{(t|\xi)}}}])^2 \quad (49)$$

$$= Var[\overline{\overline{p_{(t|\xi)}}}] - Var[E[\overline{\overline{p_{(t|\xi)}}} | \kappa]] \quad (50)$$

and therefor,

$$Var[\overline{\overline{p_{(t|\xi)}}}] = Var[E[\overline{\overline{p_{(t|\xi)}}} | \kappa]] + E[Var[\overline{\overline{p_{(t|\xi)}}} | \kappa]] \quad (51)$$

The variance cannot be negative, that is $Var[\overline{\overline{p_{(t|\xi)}}} | \kappa] \geq 0$. Therefore,

$$E[Var[\overline{\overline{p_{(t|\xi)}}} | \kappa]] \geq 0. \text{ Hence, } Var[\overline{\overline{p_{(t|\xi)}}}] \geq Var[E[\overline{\overline{p_{(t|\xi)}}} | \kappa]].$$

To reduce the modeling error using the property, it can be assumed that: the estimated model is developed with the minimum least square error; while, an infinite number of observations are provided in G (i.e., $N \rightarrow \infty$), such that the model can be precisely calibrated. In next section, this assumption will be used in our algorithm to develop the piece-wise linear model for estimating power curves using data-drive model.

3) Bias Error (B_e)

The main challenge concerning errors in estimating the power curve is to reduce the bias error. Existence of numerous zero observations and several outliers systematically impose this error in the nature of dataset G and results in deviation of the expected value of the model from the realistic value. In order to minimize this deviation,

the bias error should be reduced down to the level where the modeling error of the model does not start increasing. This can be accomplished by a recursive data cleaning technique that minimizes the bias using a benchmark obtained from the dataset with minimum modeling error.

With respect to (42), the bias error of estimating the power curve is equal to the difference between the expected output value of the model and the corresponding real-world output value. This implies that the bias error would be mitigated if this difference reduces, while the modeling error is not increasing. An efficient approach to reduce this difference is to take advantage of the Asymptotic Consistency Property (ACP) and Asymptotic Efficiency Property (AEP) ideas.

Based on these properties, as the sample size grows towards infinity ($N \rightarrow \infty$), the bias error will approach zero (i.e., ACP is satisfied), and the model will not have a modeling error/variance worse than any alternative models (i.e., AEP is satisfied). Based on our assumption, both of these properties are highly desirable in the data-driven model estimation process. They are applicable to the power curve estimation, since in this process, the size of the dataset is comprised of millions of observations. Thus, it can be assumed that N is a very large integer.

4.3 A SAS-based algorithm for estimating wind farm/turbine power curve

In this section, an algorithm is proposed to estimate the power curve with minimized modeling and bias errors. The algorithm includes two major recursive tasks:
(1) a piece-wise linear model is employed to approximate the time-series dataset of wind

power generation and wind speed; (2) outliers are removed from the time-series dataset using the piece-wise linear model as a benchmark.

4.3.1 Fitting a piece-wise linear model to dataset

The estimated model in (37) can be constructed by an approach that uses SAS to approximate the dataset G in (35) through a piece-wise linear model. To illustrate the approach, let's consider a small dataset in which there are 300 observation points (i.e., $N = 300$) and two observation variables denoted by s and p . The approach is applied to this dataset such that variable s estimates variable p differently over specific ranges of s . Figure 19 shows the scatterplot of s and p for the dataset along with the associated *B-spline* fitted to the data trend. The *B-spline* visualizes the trend of data, which helps determine the number of line segments required to model the data. Specifically, the approach for constructing estimated model based on a piece-wise linear model includes the following six major steps:

- 1) Visualizing data for trend identification: The scatterplot of correlated variables is generated for visualizing the data trend and suggesting what kind of model (e.g., piece-wise or continuous) is suitable for this data trend. In addition, by adding *B-spline*, variations in the data trend can be identified as shown in Figure 18. Knowing the points at which the data trend changes is necessary for determining the number of required line segments to model the data in the next step.

2) Determining the number of line segments and break points: Let the point at which two adjoined lines meet each other be the “break point” (c_i). At each break point the slope of the *B-spline* may be significantly different for $s < c_i$ and $s > c_i$. Thus, the approximated locations of the break points can be initially guessed with respect to the changes in the data trend visualized by the *B-spline* in step 1 (SAS would find the best break points and the other parameters independent from their primary approximated locations). Then, the number of line segments can be found based on the number of break points. In Figure 19, the possible break points are roughly located at $x = 10, 17.5, 22, 30$. Note that the approximated locations of the break points for the power curve piece-wise linear model might be in a neighborhood of cut-in speed (S_{in}) and rated speed (S_r) points.

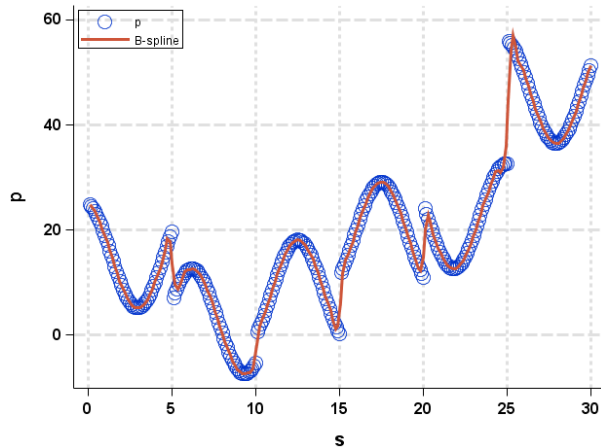


Figure 19. Scatterplot of a dataset with 2 correlated variables s and p

3) Formulating the piece-wise linear model: After the number and approximate locations of the break points are determined in step 2), the piece-wise linear function can be mathematically formulated as a system of linear equations. The

first line segment will have slope b_1 and intercept a_1 defined for the range of $s < c_1$. The second line segment will have slope b_2 , and its intercept can be defined coincided to the break point at which it meets the first line (i.e., $a_2 = c_1$). Similarly, the next line segment will have its own particular slope and its intercept can be assumed coincided to the break point between that line segment and the segment before. Thus, the piece-wise linear functions can be written,

$$p_L = \begin{cases} p_1 = b_1 s + a_1 & s < c_1 \\ p_2 = b_2 s + a_1 + (b_1 - b_2)c_1 & c_1 < s < c_2 \\ \vdots \\ p_i = b_i s + a_1 + \sum_{i=1}^{i-1} c_{i-1}(b_{i-1} - b_i) & c_{i-1} < s < c_i \end{cases} \quad (52)$$

- 4) Finding initial values for unknown parameters: In the piece-wise linear functions in (52), there are unknown parameters (i.e., intercept, slopes and break points), which should be fitted to the data trend. Let “ θ ” denote a set comprising the unknown parameters that exist in (52). Initial values of these parameters in θ can be approximately guessed using the scatterplot of step 1. Note that providing an initial guess facilitates the starting points in the SAS non-linear parameter estimation process, since specifying the first and the second order derivatives of the non-linear model equation with respect to the parameters can be avoided.

- 5) Estimating the best fit for the parameters in set θ : To estimate the best fitted values for the parameters in set θ , an iterative non-linear regression technique will be used to improve the initial values with respect to the data trend. As the relation between the predictor and the outcome variables is non-linear, the

regression model should be non-linear as well. This model estimates the parameters using a non-linear least squares technique, which involves searching for those values in the parameter space that minimize the residual sum of squares. Specifically, the parameter estimation using a non-linear regression model is an iterative process in which the initial values in set θ are being used as the starting points. To carry out the iterative calculations, the SAS non-linear regression modeling function is an appropriate tool, which can be used for managing big datasets. It can be utilized to solve non-linear least squares problem by different numerical calculation methods, such as *Gauss-Newton* method. This method uses derivatives/approximated derivatives of the sum of squares error with respect to the parameters to lead the searching process to the direction in which the parameters producing the smallest sum of squares error. When the convergence criterion defined in SAS is met, the best fitted values for the parameters of set θ can be substituted in (52).

- 6) Creating a new dataset for linear regression analysis: At this step, the SAS Simple Linear Regression (SLR) procedure is used to create a new dataset for enhancing the accuracy of estimated model. The SLR function is used to find the predicted values of p_L function (i.e., \bar{p}_L) for all ranges of s by fitting approximated values of p_L more precisely to the data trend. To this end, a new dataset (*tmp*) should be created in which values of all p_i s are included as variables,

$$tmp = \{p_L | p_i \text{ for all } s \text{ ranges}\} \quad (53)$$

Then, the SLR procedure can be used to run regression analysis on this dataset to generate and store the predicted values of p_L over all ranges of s . Figure 20 shows the obtained 4-segment piece-wise linear model associated with the sample dataset presented in Figure 19. The obtained \bar{p}_L includes the final values of the estimated piece-wise linear model fitted to dataset G .

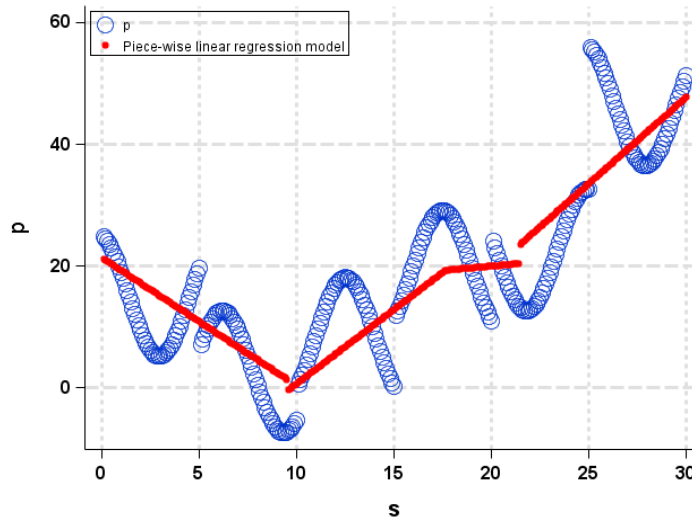


Figure 20. A piece-wise linear model fitted to the dataset

4.3.2 Data Cleaning for Bias Error Reduction

When the above approach for constructing estimated model based on a piece-wise linear model is applied to dataset G in (35), the final model can be considered as the linear approximation of the power curve. However, it may involve imperfections due to linearizing approximations and bias errors, which can be reduced by another approach for cleaning bias errors out in the dataset, which uses the developed piece-wise linear model as a benchmark. In the cleaning process, modeling errors for estimating an accurate power curve are also cleaned out in addition to bias errors.

The cleaning process is based on ACP and AEP. Specifically, the process includes the following four steps:

Step 1. An estimated piece-wise linear model for dataset G in (35) is developed as the benchmark (i.e., \bar{p}_L).

Step 2. A significant percent (15%-25%) of the elements in $G = \{(s_i, p_i) | i=1, \dots, N\}$ are associated with zero wind speed ($s_i = 0$). In order to reduce the variance in models obtained from G , most of these zero elements are removed from the dataset. Furthermore, outliers with a non-zero recorded value of s_i are eliminated. The elimination criterion for these undesirable observations can be explained as follows,

Elimination Criterion: It can be shown that for large N values at least λ percent of the observations in G are distributed in ρ standard deviations from their associated \bar{p}_L line segments. Thus, if an observation in G is excluded from the interval η , it can be eliminated as an outlier. λ and η are defined as follows,

$$\lambda = (1 - \frac{1}{\rho^2}) \times 100 \quad (54)$$

$$\eta = (\bar{p}_L - \rho \sigma, \bar{p}_L + \rho \sigma) \quad (55)$$

where ρ can be determined based on the particular distribution of G , which can be simply visualized with a histogram. However, with respect to the Empirical Rule, $\rho = 2$ would be sufficient enough to include about %95 of the distribution.

Proof: Let S_k be the set of observations (p_j) of G that are distributed in ρ standard

deviations from $\overline{p_L}$. That is,

$$S_k = \{j : 1 \leq j \leq N; |p_j - \overline{p_L}| \leq \rho\sigma\} \quad (56)$$

With respect to variance definition, deviation of p_j 's from $\overline{p_L}$ can be written as follows,

$$(N-1)\sigma^2 = \sum_{j=1}^N (p_j - \overline{p_L})^2 \quad (57)$$

$$= \sum_{j \in S_k} |p_j - \overline{p_L}|^2 + \sum_{j \notin S_k} |p_j - \overline{p_L}|^2 \quad (58)$$

Observe that in (58) the data is divided into two sets. One set contains those samples that lie within the $\rho\sigma$ tube around the estimator; and the other set comprises the remaining points outside the tube. In (58), both terms are positive; so, by ignoring the samples inside the tube expression (58) can be rewritten in the following form,

$$(N-1)\sigma^2 \geq \sum_{j \notin S_k} |p_j - \overline{p_L}|^2 \quad (59)$$

$$\geq (N - N_{(S_k)})\rho^2\sigma^2 \quad (60)$$

It is desired to find an expression for the percentage of samples in the tube. By doing some manipulations in (60), the ratio of the number of observations included in S_k to the number of total observations in G would be equal to,

$$\frac{N_{(S_k)}}{N} \geq 1 - \frac{1}{\rho^2} + \frac{1}{N\rho^2} \quad (61)$$

Since the number of observations in G is commonly very large, the third right hand side term can be ignored. Thus, (61) can be written as follows,

$$\lambda \geq 1 - \frac{1}{\rho^2} \quad (62)$$

Step 3. A new dataset (ω_k) should be created in which only observations within η are stored. That is,

$$\omega_k = \{p_i \mid p_i \in (\bar{p}_L - \rho\sigma, \bar{p}_L + \rho\sigma)\} \quad (63)$$

Step 4. The dataset ω_k should be examined that if it meets the convergence criterion of the recursively cleaning process to stop, and introduce ω_k as the estimated power curve dataset. The convergence criterion is met when no more outliers can be eliminated from the most updated ω_k . Otherwise, the recursively cleaning process should be repeated from *Step 5* for the most updated ω_k until the convergence criterion is met. Note that the initial values for parameters in set θ are not needed to be calculated and updated by user for each recursion. They will be the estimated values from the previous recursion; however, the SAS non-linear parameter estimation procedure will improve them with respect to the most updated dataset.

The proposed algorithm includes two major recursive tasks, 1) fitting a piece-wise linear model to the time-series wind power generation-wind speed data trend, and 2) cleaning modeling and bias errors recursively using the piece-wise linear model as a benchmark. The algorithm is used to estimate the power curve from real-world data while minimizing the modeling error and bias error simultaneously. The final cleaned dataset and the associated piece-wise linear model can be utilized to assess the wind turbine/wind farm operation, such as future generation forecast for reliability assessment, fatigue analysis, or efficiency evaluation studies.

Figure 21 shows a flowchart in which the steps of power curve estimation using this algorithm are presented.

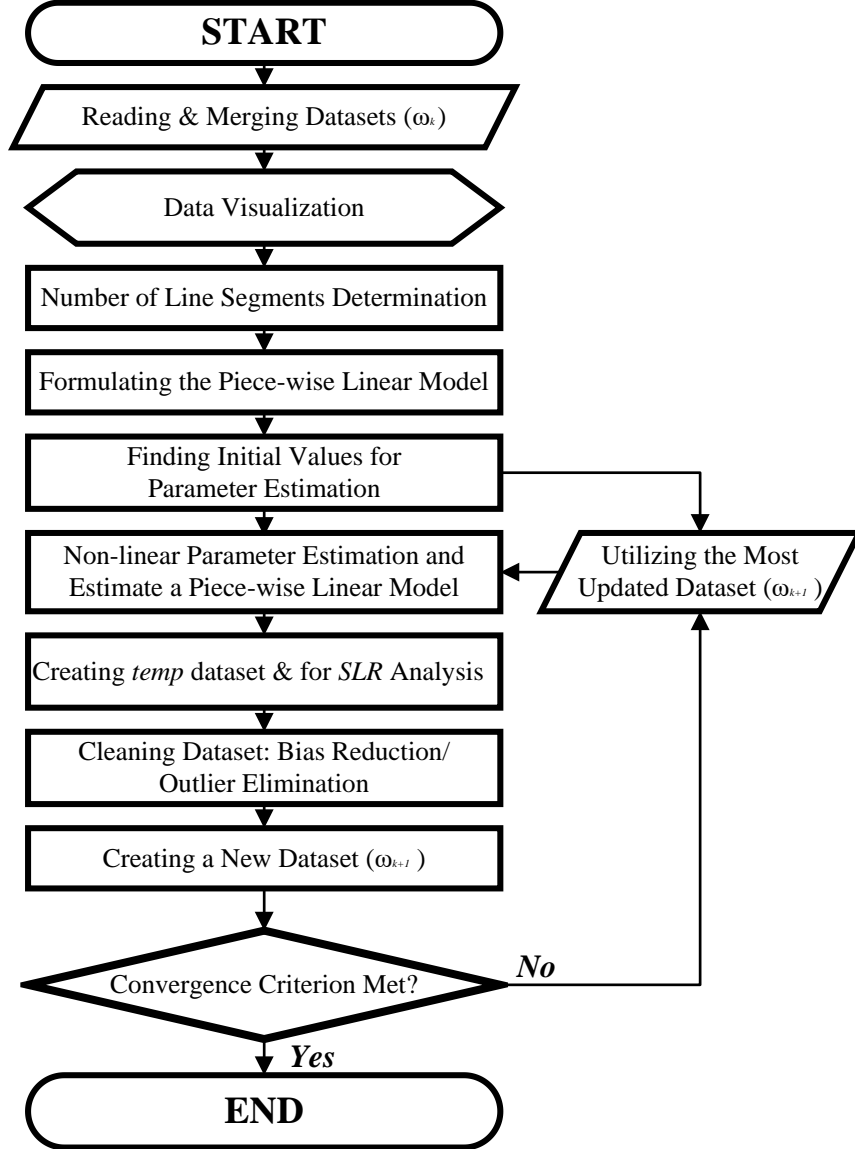


Figure 21. Flowchart of the recursive algorithm for power curve estimation

To further illustrate how the algorithm cleans a dataset, let's consider the mock power curve presented in Figure 22. In this figure, the outliers are deliberately exaggerated for the sake of illustrating the order of outlier elimination for each recursion

of the algorithm. By applying the algorithm to this raw dataset, after 5 recursions the convergence criterion is satisfied. In this figure, the numbers on data points show the recursion numbers. It can be seen that in each recursion, observations excluded from $\bar{p}_L \pm \rho \sigma$ are identified as outliers and eliminated until no more observation outside of $\bar{p}_L \pm \rho \sigma$ exist (i.e., the 5th recursion).

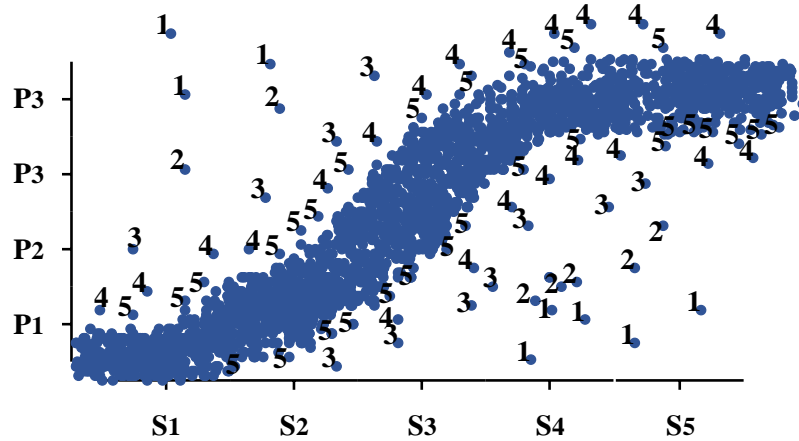


Figure 22. A mock power curve on which the order of outlier elimination for each recursion of the algorithm is shown

This algorithm can be used to estimate the power curves based on the actual dataset of wind power generation and wind speed while simultaneously minimizing both the modeling and bias errors caused by outliers in the dataset. In the algorithm, a continuously updated piece-wise linear model is used to minimize modeling errors while bias errors are reduced by using SAS software package to recursively clean outliers out in the real dataset. As a result of being SAS-based, the algorithm is designed to be self-adaptive, which makes it applicable to a variety of datasets including any kind of bias or undesirable observations. In addition to power curves, the proposed algorithm can also

provide cleaned dataset and the associated piece-wise linear model for various operation assessment purposes, such as efficiency and fatigue analysis studies.

Chapter 6: Estimation of Solar PV Plants Power Generation Drops

Based on Clouds Distribution

In this chapter, the main challenge of solar power generation that is sudden drops of power generation is discussed. An approach is developed to deal with this challenge through estimating the drops of solar PV plants power generation based on clouds distribution. The validity of the approach is confirmed by comparing the associated results against the cloud data collected by satellite.

6.1 Solar power generation

Solar power from solar PV plants (photovoltaic panels) is a renewable resource of clean energy and it changes with variations of weather condition. The term “photovoltaic” comes from the Greek, which is *phos* meaning light, and *voltaic* from the name of the Italian physicist *Volta*, after whom the unit Volts is named. The modern era of solar power generation began back in 1954 when *Bell Laboratories* discovered that silicon doped with certain impurities was able to generate electricity for satellites, [48]. Afterwards, power generation entities used photovoltaic panels to generate clean power in utility-scales. For example, Figure 23 shows a solar PV plant by the National Renewable Energy Laboratory (NREL) near Tonopah, Nevada, which has an electricity generating capacity of 110MW, [49].

When photons hit the solar PV panels, they are absorbed by semiconducting materials, such as silicon, and create a $V - I$ source to extract energy from. When a photon is absorbed by the solar PV panels, its energy is given to an electron-hole pair in

the crystal lattice. The electrons and holes have to move to the collection electrodes of the solar cell to create a $V - I$ source. This way, the solar PV arrays convert solar energy into DC power. Then power electronic devices such as converters invert the DC power to AC to feed the transmission/distribution system.



Figure 23. Arial and close views of a 110MW solar PV plant in the state of Nevada

6.2 Reliability challenge of solar power generation

The most challenging operating condition in solar power generation happens when passage of a cloud bank significantly reduces the solar irradiance, which results in sudden and large variations in the solar PV plant output, [50], [51]. This operating condition can become even more critical if passage of a cloud bank takes place with a sudden change of load. Under such operating conditions, the system operator has to deal with these variations with either redispatching the synchronous generators or importing power from the adjacent control areas. The impact of solar PV plants on the power grid operating condition varies from one to another, since operating condition of a power grid is dependent on its generation mix, ramping rate limits, ability to respond to variations of load/generation, etc.

In operating a power grid integrated to several solar PV plants, it is very important to accurately forecast the solar power generation, and specifically the moments when sudden generation drops may happen. Estimation of solar PV plants performance is typically based on stochastic processes with weather related variables, such as clouds distribution, solar irradiance, temperature of photovoltaic panels, etc. that makes an accurate estimation difficult. Among all these variables clouds distribution plays a key role in estimation of solar power generation. Since clouds distribution severely impacts the solar irradiance, which is the most dominating factor in operation of solar PV plants.

There are various clouds distribution that can affect the solar power generation through casting a shadow over the solar PV arrays, [52]. They are mostly characterized by their size, shape, speed, direction and optical transmission. Each cloud distribution allows a specific amount of solar irradiance reach to the earth surface during a certain

period of time/day/season. Hence accurate estimation of solar power generation drops requires forecasting the clouds distribution over the solar PV plants.

6.3 Impact of clouds distribution on solar power generation drops

It becomes more and more clear that distribution of output level and dramatic variation of solar PV generation will impact the grid reliability and voltage stability. Particularly in a high penetration scenario, a better forecast of solar power generation is very important for reliability management and operation. This research is to investigate the impact of distribution and variations of clouds on solar irradiance, and thus the output level and sudden drops of solar power generation.

More specifically, the goal is to know if knowledge of cloud distribution can improve the forecast of solar power generation drops to better understand the impact of solar power generation on voltage stability and/or quality of electricity services. In recent impact analysis of renewable resources, some system operators such as ERCOT and GE gauge their voltage stability and/or quality of electricity services by system strength evaluation. System strength evaluation may show the system ability to remain stable and maintain the quality of load service following variations in solar PV generation. It is commonly measured by an extended usage of Short Circuit Ratio (SCR). There are a number of major operational factors that may significantly impact the system strength at the point of interconnection of solar PV plants,

- Point of interconnection (location) of solar PV plants to the power grid,
System strength may have different “stability implication/reflection” at different locations of the system, i.e., load buses/Points of Interconnection (POIs).

- Rate of change of solar PV generation,

A solar PV plant is a solid-state system in which the variations of generation can be dramatic. It is observed that some variations in solar generation output are similar to sudden changes of load, such as failures or faults.

- Reactive power support sufficiency at POIs,

Solar PV plants are non-synchronous/solid-state generation units, which are power electronics connected and provide significantly lower reactive support for voltage stability compared to synchronous generators.

A change in any of these factors may cause significant variations in the system strength. Variation of system strength directly affects the voltage stability and power quality of the system. Thus, it is important to evaluate the variations of system strength under real-world operating condition of solar PV plants, which includes sudden generation drops due to variations of clouds distribution. Currently, there are a few methods/measures to evaluate the variations in the system strength at the point of interconnection of solar PV plants. These measures consider the full-capacity of a solar PV plant to evaluate the variations in the system strength at a point of interconnection. Using the full-capacity of a solar PV plant (i.e., assuming a plant is generating either

0MW or at its maximum capacity) is a too conservative assumption that may result in misleading or even unrealistic results for high penetration scenarios. The evaluation results would be more precise if the real-world operating condition of the solar PV plant can be used instead of using its full-capacity. More precise results will provide insights about sudden solar power generation drops that is a major concern for electric utilities.

6.4 Impact of clouds distribution and solar power generation drops on system strength

System strength at the point of interconnection of a solar PV plant is dependent on the amount of solar power generation at each moment of operation. A sudden drop of solar power generation of a solar PV plant may vary the system strength not only at its point of interconnection, but also at other locations in the system. Hence, system strength is dependent on intensity of solar power generation that varies with the weather and sun's position with respect to the solar PV panels. To more accurately estimate the system strength, it should be estimated based on realistic amount of solar power generation. Solar power generation is highly correlated with the solar irradiance and clouds distribution, [51].

Variations in the system strength is indirectly but strongly affected with the cloud distribution. As suggested by the meteorologists, clouds distribution is different at various geographical locations and dependent on the variations in the form of clouds. It is known that clouds distribution and the level of solar radiation are highly correlated, which implies solar irradiance may also suddenly vary at various geographical locations. Solar irradiance plays a critical role in operating condition of the solar PV plants. The operating

condition is characterized by the rate of solar power generation change and the distribution of output level that both have significant impacts on the results of SCR-based measure (i.e., SDSCR) for system strength evaluation. Figure 24 shows how clouds distribution can impact the variations of the system strength.

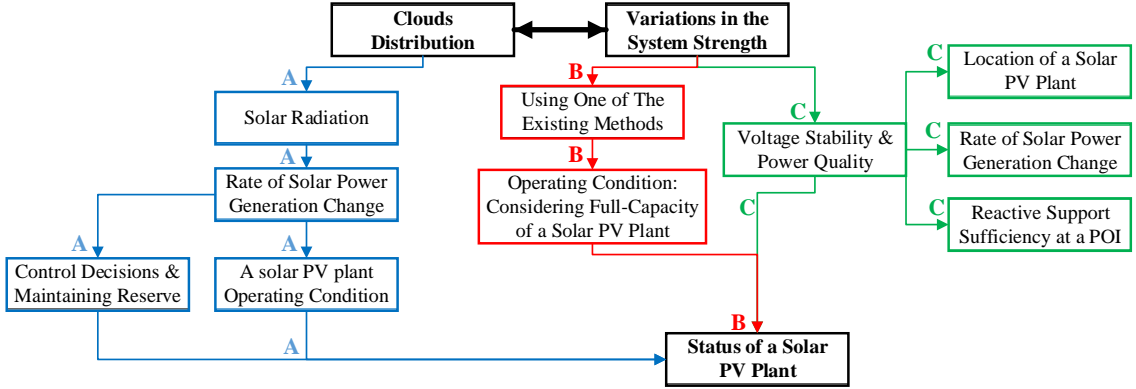


Figure 24. Relation between system strength and the cloud distribution

In real-world operation, clouds distribution affects the system strength by varying the solar PV generation (i.e., solar PV plant operating condition). To illustrate it, let's consider evaluating the system strength using the SDSCR measure introduced by Equation (31). In this equation, P_i would be traditionally equal to the full-capacity of the solar PV plant. This is a common assumption that electric utilities and solar/power grid operators have for system strength evaluation. However, in real-world operation, P_i that is the amount of solar power generation/drop at the point of interconnection i is often not equal to the full-capacity due to the variations of solar irradiance caused by the movement of clouds with different distributions.

Thus, the more accurate estimation of solar PV generation would be P_i^* , which can be estimated with respect to different modes of clouds. Similarly, $V_{(i)}$ would be the

function of P_i^* that is the estimated amount of solar PV generation/drop at the point of interconnection i . Using the realistic values of P_i and $V_{(P_i)}$ estimated based on the clouds modes, equation (31) can be re-written as follows,

$$SDSCR_i = \frac{|V_i^*|^2}{P_i^* + \sum_{j \in \mathbf{R}, j \neq i} P_j w_{ij} \cos \alpha_{ij} |Z_{RR,ii}|} \quad (64)$$

Equation (64) will evaluate the system strength at the point of interconnection of a solar PV plant more accurately based on realistic solar power generation/drop estimation obtained using clouds distribution. To obtain this information, an approach is required to forecast the clouds distribution.

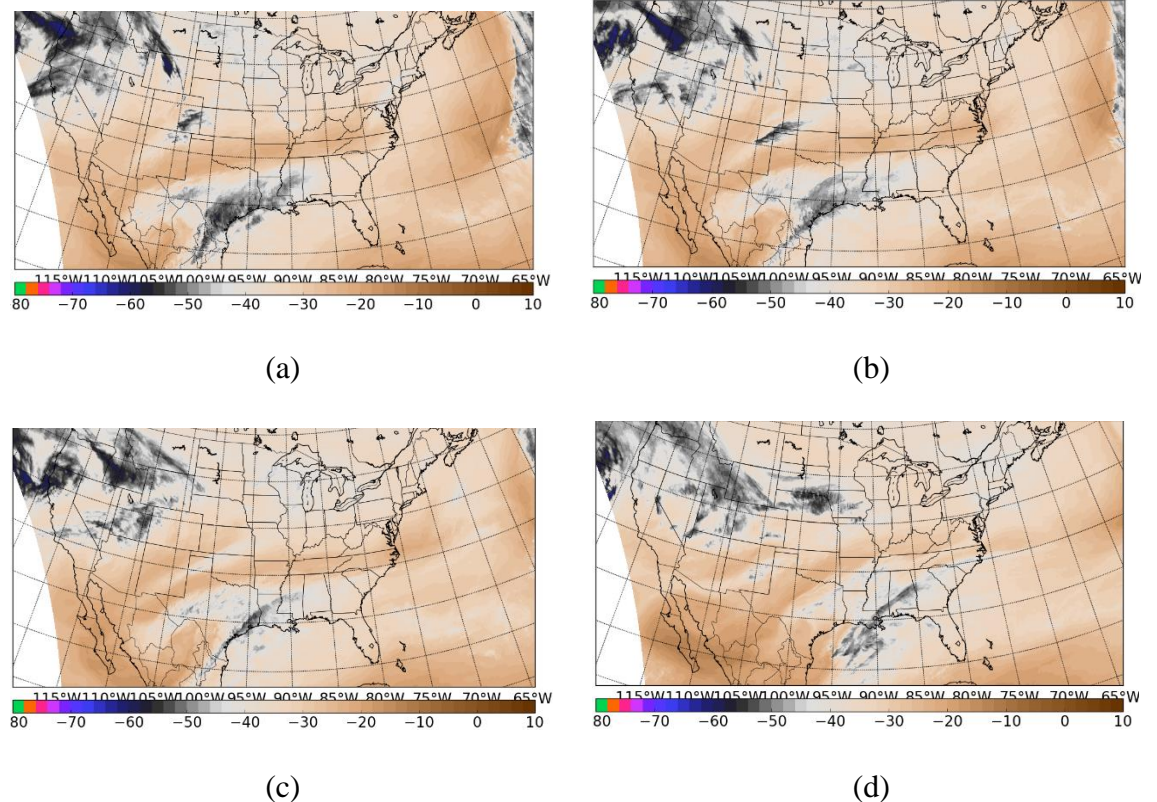
6.5 Estimation of clouds distribution

An approach is developed to forecast the clouds distribution using historical weather data. The approach utilizes a time-series dataset including several weather parameters around the solar PV plant of interest. This dataset is used to train and validate an Artificial Neural Network (ANN) model that forecasts the solar irradiance based on the weather parameters. Given a big dataset including all the important weather parameters as the input of the ANN model, it's expected that the model can precisely forecast the solar irradiance. However, an important missing parameter in the ANN model input dataset imposes an error in the solar irradiance forecast results.

The weather scientists believe that the missing parameter is the cloud information. In other words, existence of clouds cause forecasting error in the ANN model output. Thus, it can be assumed that the forecasting error of solar irradiance forecast using a ANN model at each time interval is caused by the clouds at that time interval. Hence, the

approach considers the ANN model's solar irradiance forecast error as an indication of cloud information. As the shape/sparseness of clouds includes a high degree of uncertainty, this approach identifies the status of clouds in terms of various modes. This way, significant changes in clouds distribution can be identified based on change of clouds mode from one to the other. (The clouds modes are introduced in the following subsection 6.5.1).

The validity of the developed approach and this idea is verified by visualizing the satellite collected "condensed moisture/cloud" data⁶ shown in Figure 25. This Figure shows how clouds distribution changes over each state in the United States territory.



⁶ The cloud information is provided by the *National Weather Center* (NWC), Norman, Oklahoma and *National Oceanic and Atmospheric Administration* (NOAA).

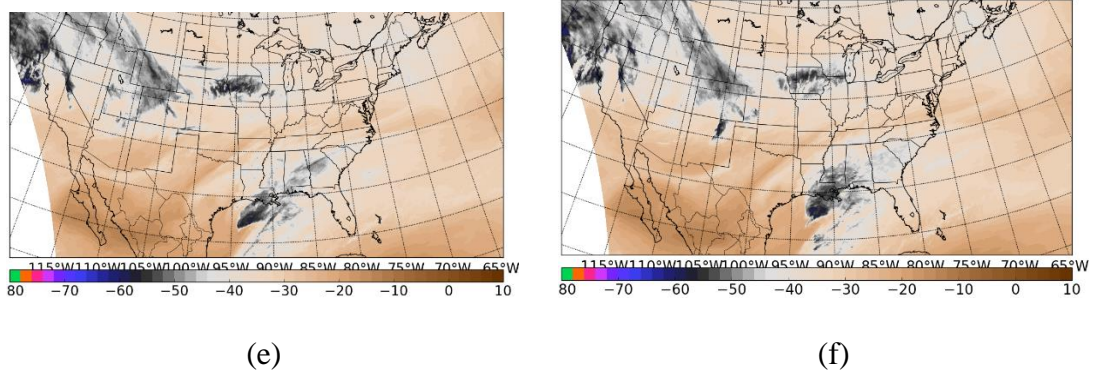


Figure 25. Pictures (a)-(f) show clouds distribution over the United States

6.5.1 Definition of cloud modes from power system operation perspective

In meteorology science, there are many different criteria for clouds classification.

As the most common criterion suggests, clouds can be classified into three general types with respect to their altitudes, i.e., low-level, mid-level and high-level. Within each general type, additional classifications are also defined based on clouds appearance/sparseness, i.e., *Cirrus* (meaning hair like), *Stratus* (meaning layer), *Cumulus* (meaning pile) and *Nimbus* (meaning rain producing). These classifications are defined based on specific requirements of studies performed in weather/meteorology science not for representation of sudden variations of the solar radiation level, which is a critical concern in power system operation.

From the power system operation perspective, four cloud modes are defined such that change of clouds mode from one to another-caused by their movement-may result in sudden variations of the solar irradiance and therefore solar power generation/drop. The four cloud distribution modes defined for this study are (i) clear, (ii) partly clear, (iii) partly cloudy and (iv) cloudy. These four modes can be used to estimate the sudden solar power generation drops forecasted using the proposed approach.

6.5.2. An approach of estimating clouds distribution

The developed approach prepares the historical weather data and utilize it for training an ANN model to forecast the solar irradiance. Then it uses the forecast error to identify the clouds modes for each time interval of interest, and verify it with the previous satellite collected clouds data (if available). The approach is mainly comprised of the five following steps,

- Cleaning and preparing historical weather data,

The basic requirement of this approach is historical weather data. This dataset is commonly a 5-minutes time-series data including information on time, date, air temperature, wind speed, wind direction, maximum wind speed, solar irradiance, rain, air pressure and relative humidity. It includes several missing values and outliers that are needed to be removed from the data.

In particular, the solar irradiance includes several zero observations for the evening and night times. In this study, these observations are considered as outliers and needed to be eliminated from the dataset.

- Creating sun position variable in dataset,

As discussed before, position of sun in the sky plays a very important role in the amount of solar irradiance received on the solar PV panels. Hence, a variable should be defined as the “index for the position of sun in the sky”. This index can be created using the hour portion of time variable such that a number from 1-24

is assigned to each row of 5-minutes data with respect to the hour portion of time.

This way the weather data will be ready for training the ANN model.

- Training, validating and testing an ANN model using historical data,

An Artificial Neural Network (ANN) maps between a dataset of numeric inputs and a set of numeric targets/outputs. The historical weather dataset is utilized to train and validate a ANN model. In this model, all the variables in the dataset will be used as the input but the solar irradiance. The solar irradiance will be used as the output for training the model.

To train the ANN model several software packages can be used such as SAS or MATLAB. In this study, MATALB is used to train, validate and test the ANN mode. It easily helps select data, create and train a network, and evaluate its performance using mean square error and regression analysis.

- Forecasting solar irradiance and obtaining the forecast error,

By training and validating the ANN model, the forecast error for the solar irradiance forecast can be also calculated. This error is used as an indication of clouds distribution over the location where the solar PV plant of interest is located.

- Identifying the clouds mode for each time interval,

In this step, the forecast error obtained from the previous step is being used to identify the clouds mode for each time interval. To this end, the absolute values of the forecast errors are sorted in the ascending order. Each quartile of the sorted

errors will be assigned to a cloud mode as described in Table 2. Based on the relation shown in this Table, the smallest forecast errors are associated with clear moments, and the largest forecast errors are associated with cloudy moments. In other words, big values of forecast errors denote cloudy moments over the solar PV plant.

Table 2. Relation between clouds modes and quartile numbers	
Quartile Number	Cloud Mode
1	Clear
2	Partly clear
3	Partly cloudy
4	Cloudy

- Verifying the results using satellite cloud data,

After identifying the clouds type, the accuracy of the results can be verified using the condensed moisture/clouds data that is routinely collected by the weather satellites. The satellite data is needed to be translated into visualized pictures in order to compare the cloud types at each moment identified by the approach with the clouds distribution informed by satellite.

6.5.3 Approach Illustration using simulation study

To further illustrate the developed approach and demonstrate its practical applicability, the approach is implemented to estimate the clouds distribution over a solar PV plant located in central Oklahoma. To this end, a big time-series dataset including

several weather parameters collected at 9 weather stations around a solar PV plant is used. The weather stations are shown in on Oklahoma map in Figure 26.

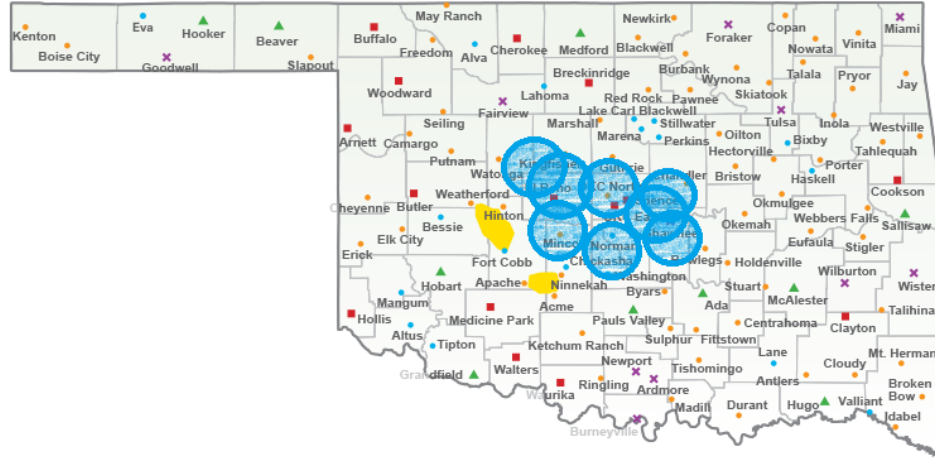


Figure 26. Map of Oklahoma state with the 9 weather stations

More specifically, this dataset is utilized to train and validate an Artificial Neural Network (ANN) model that forecasts the solar irradiance based on the weather parameters explained in subsection 6.5.1. For the sake of simplicity of illustration, the focus of this simulation study is on a particular day, that is February 23, 2015. In this day, the sunrise was at 13:08:00 UTC/07:08:00 CST. This dataset is comprised of time (TIME), relative humidity (H), air temperature (T), Wind speed (SPD), wind direction (DIR), max wind speed (MAX), rain (RAI), solar irradiance (SR), hour (HO), air pressure (P) and sun position index (SDX). The top five rows of this dataset are shown as a sample in Table 3.

This dataset is used to train an ANN model that receives all these variables but the solar irradiance as an input and forecasts the solar irradiance as the output.

Table 3. Sample of central Oklahoma weather dataset

TIME	H	T	SPD	DIR	MAX	RAI	P	SR	HO	SDX
23FEB2015:13:00	78.22	-7.37	6.27	19.44	8.28	0	993.9	0.00	13	1
23FEB2015:13:05	78.00	-7.38	5.91	19.56	8.51	0	993.9	0.22	13	1
23FEB2015:13:10	77.89	-7.38	6.24	15.22	8.71	0	993.9	0.56	13	1
23FEB2015:13:15	77.44	-7.38	6.71	17.11	9.11	0	994.0	0.89	13	1
23FEB2015:13:20	76.89	-7.39	6.54	18.22	8.91	0	993.8	2.33	13	1

After training an ANN model and finding the forecasting errors, for each 5-minute time interval a cloud mode (i.e., cloud distribution) is identified. The biggest forecast errors, which are located in the fourth quartile are identified associated with cloudy moments of the day. The results are shown in Table 4 below⁷.

Table 4. Results of clouds distribution forecast

Time	Forecast Error	Cloud Mode
18:00:00	374.32	Cloudy
18:30:00	372.58	Cloudy
17:30:00	347.90	Cloudy
19:30:00	339.88	Cloudy
19:00:00	334.61	Cloudy

To verify the accuracy of the results obtained from the approach, the condensed moisture/cloud data over Oklahoma obtained from the satellite is visualized and shown in Figure 27. In addition, Figure 28 shows the variations of solar irradiance over central Oklahoma on February 23 2015. As it can be seen from this Figure, the solar irradiance over this particular part of the state was significantly dropped at 17:30-19:30 UTC.

⁷ Due to the fact that satellite data resolution is 30-minutes, the resolution of the data is reduced from 5-minutes to 30-minutes for the sake of comparison.

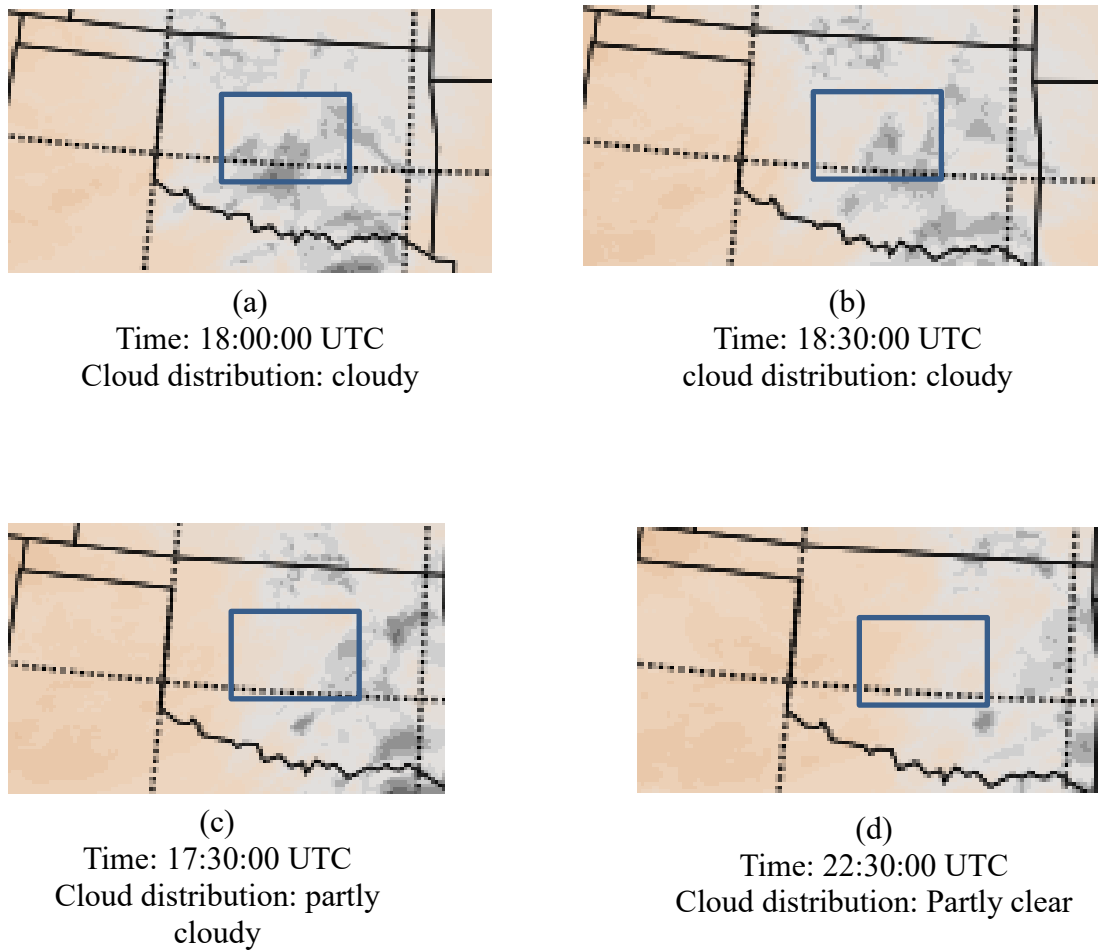


Figure 27. Clouds distribution over state of Oklahoma obtained from satellite data

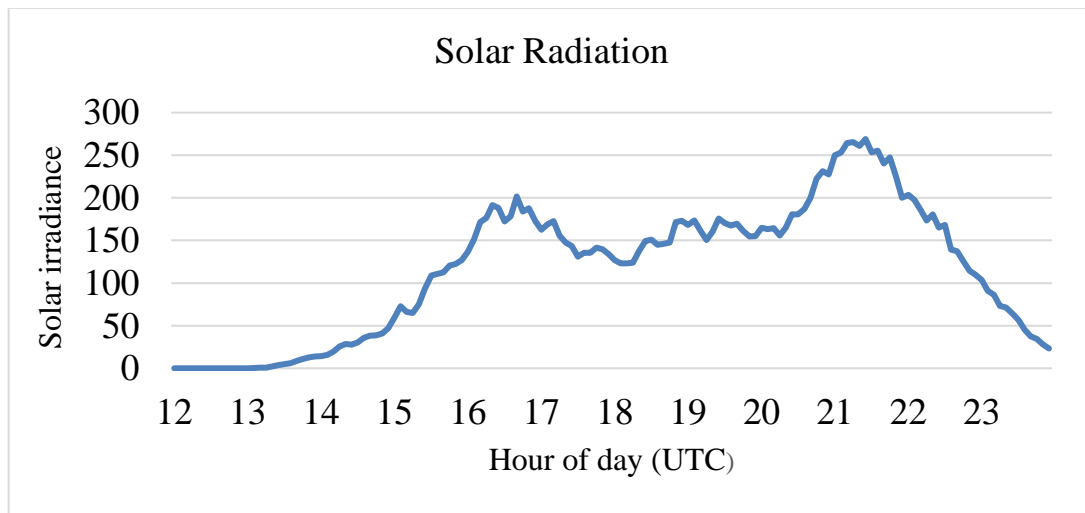


Figure 28. Solar irradiance on February 23, 2015

As it can be seen from comparing Table 4 with Figure 27 and Figure 28, the results of the clouds distribution obtained from the developed approach is agree with the cloud distribution information from the satellite data. More specifically, in Figure 27 and Figure 28 the solar irradiance over this particular part of the state was significantly dropped at 17:30-19:30 UTC, which implies during that time it was cloudy in central Oklahoma. This is what exactly shown by the results of the cloud distribution study performed using the new approach. Based on the results presented in Table 4, the cloudiest moments of February 23, 2015 were at 17:30-19:30 UTC, which is agree with reality (satellite data).

6.6 More precise evaluation of system strength for solar PV plants

After demonstrating the relation between clouds distribution and the system strength, more accurate system strength evaluation based on clouds distribution (i.e., the estimated values of P_i^* and V_i^* for the current or predicted cloud mode) can be perform through the four following phases,

- Using the developed approach to forecast the clouds distribution in the area where the solar PV plant is located,
- Using the cloud forecast information to determine the cloud modes for each time interval,
- Using the cloud modes to estimate the realistic solar PV plant operating condition (i.e., P_i^* and V_i^*) associated with the distribution of output level and rate of solar PV generation change,
- Evaluating the system strength in terms of voltage stability using the developed enhanced measure, i.e., SDSCR.

By using this approach, the system strength can be evaluated closer to the actual conditions of critical areas of interest with better understanding of cloud modes and the impact of clouds on dramatic changes of solar power generation. Moreover, the improved understanding of system strengths obtained from cloud distribution forecasting is beneficial to the power system operators. Since it helps them make more appropriate decisions in control and maintaining sufficient reserves, which will affect dispatch decisions, thus overall economic efficiency and reliability of the grid.

Chapter 7: Identifying Combination of Weakest Points of Interconnection Using Structural Analysis

In this chapter, the goal is to identify a group of buses (points of interconnection) that integration of renewable resources to all of them results in the lowest system strength. To this end, power grid structural properties of the SDSCR measure is used to efficiently identify the combination of weakest points of interconnection with respect to the real electrical connectivity of them. The outcome of this analysis provides beneficial understanding about the system strength for the power system planning and integration of renewable resources studies.

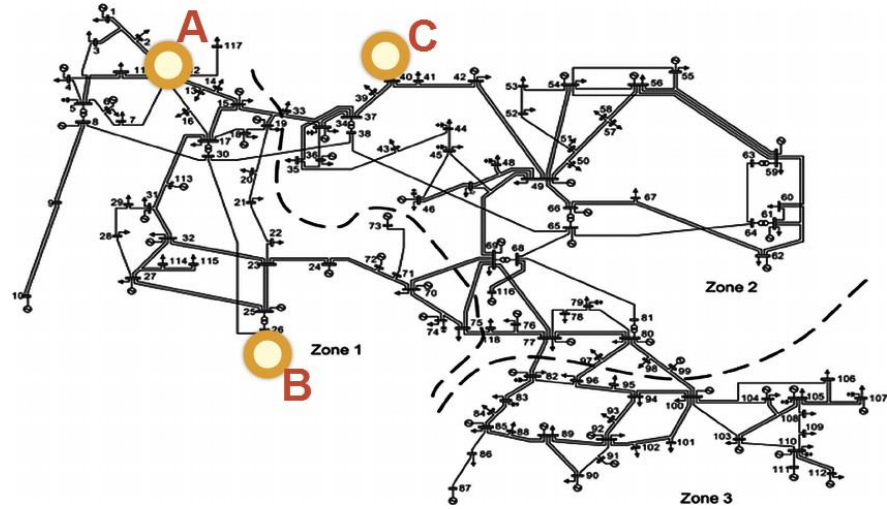
7.1 Weakest point of interconnection

Interconnection of a renewable source to the power grid makes it weaker due to the uncertainties involved in renewable generation and lack of sophisticated voltage stability support. When several renewable sources are interconnected to the power grid (i.e., high penetration scenarios), the power grid becomes significantly weaker. Under such operating conditions, identifying the weak points of interconnection is of high importance, since it helps the power grid operator avoid serious operational difficulties. The SDSCR measure can be used for evaluating the system strength at all points of interconnection in order to identify the buses with the lowest system strength values as the weak buses.

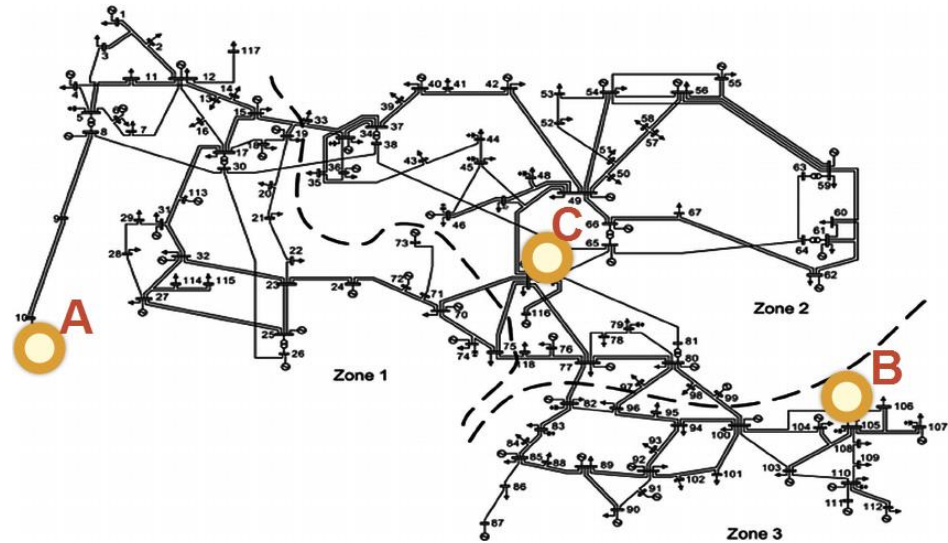
This way of using the SDSCR measure for identifying the weak points of interconnection provides practically accurate results at the stage of operation where the

locations of all renewable resources are known. While at the stage of planning, the goal of studies is to identify (a) appropriate locations for integration of multiple renewable resources, and (b) the group of weakest points of interconnection, from the system strength perspective. At the stage of planning where the locations of all future renewable resources are not known, the SDSCR measure cannot be directly used to identify the group of weakest points of interconnection. Since interconnection of a certain generation capacity of renewable resources to different locations would result in different system strength at each point of interconnection. In other words, interconnecting a number of renewable resources to different combinations of locations results in different system strengths.

To further illustrate the important impact of different configurations of renewable resources on the system strength consider Figure 29. It shows two scenarios of integrating three 100MW renewable resources (i.e., wind farms *A*, *B* and *C*) to different points of interconnection in the IEEE 118-bus transmission system. The only difference between the two scenarios is in the locations (points of interconnection) to where the three wind farms are interconnected. In the first scenario, the wind farms are electrically closer to each other with a specific configuration, while in the second scenario, the wind farms configuration is different and they are electrically farther. In both scenarios of integration, 300MW of wind power is integrated to the transmission system; however, the system strength at the points of interconnection in the first scenario are lower due to a different configuration. This simple example shows the importance of choosing appropriate locations for integration of multiple renewable resources.



(a) first scenario of integrating three renewable resources



(b) second scenario of integrating three renewable resources

Figure 29. IEEE 118-bus power transmission system with three renewable resources interconnected to different locations in two scenarios

In scenarios 1 and 2, the weakest buses are not identical due to different points of interconnection of renewable resources. Integration of certain amount of renewable power generation to various locations in the system will result in different system strength values at their points of interconnection.

7.2 Challenge of identifying weakest combination of points of interconnection

Each combination of points of interconnection may introduce a particular group of weak buses. It implies that finding the weakest points of interconnection requires studying the system strength for integration of renewable resources to all possible combinations of buses. More precisely, in order to identify the weakest points of interconnection for integration of n_r renewable resources to a power grid with n potential point of interconnection (i.e., buses), the system strength evaluation study is required to be performed for $C_{n_r}^n$ combination of points of interconnection. Equations (64) and (65) shows the combinatorial nature of the problem.

$$\frac{(\# \text{ of potential POIs})!}{(\# \text{ of renewables})! [\# \text{ of potential POIs} - \# \text{ of renewables}]!} \quad (65)$$

$$= \frac{n!}{n_r! * (n - n_r)!} \quad (66)$$

To perform the study through exhaustive search, all possible combinations of points of interconnection should be studied, which is extremely time consuming. To illustrate it, here is an example of study of finding the weakest combination of points of interconnection in a large-scale power grid. In this study, 4 stressed scenarios are defined for 69kV, 34.5kV, 13.8kV and 13.2kV voltage levels. In each scenario, 3 cases of renewable resource integration are considered. Figure 30 shows the scenarios and the cases of integration defined for this study. For each stressed scenario and case of integration,

- System strength is evaluated for all load and transfer buses,
- Groups of weakest and strongest buses in terms of system strength are identified,

- Potentially appropriate zones for integration of solar PV plants are identified.

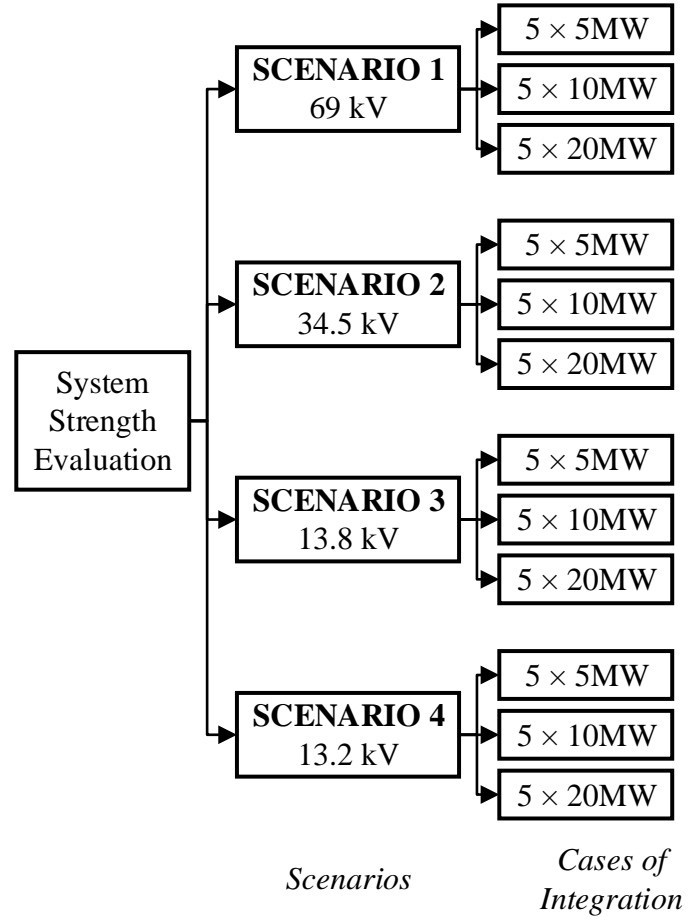


Figure 30. Stressed scenarios of renewable resource integration study

More specifically, in this study the following two steps are followed:

- Step1
 - a renewable resource (e.g., solar PV plant) is interconnected to each bus,
 - power flow is solved and SDSCR method is used to evaluate the system strength at all of the buses,
 - a group of weak bus candidates is determined.

- Step 2
 - system strength is evaluated for integration of solar PV plants to all x combinations of the weak bus candidates,
 - two groups of buses with lowest and highest SDSCR measures are identified as the weakest and strongest points of interconnection.

As it can be seen from (64)-(65) and the steps above, curse of dimensionality is the major challenge of identifying weakest combination of points of interconnection. In the study above several simulation studies are needed to be performed, which may require several hours of execution and supercomputers for large scale system, such as ERCOT power grid. For example, the number of combination is 2,118,760 even when the number of potential point of interconnection is 50 and the number of renewable resources is only 5. Normally, this problem is hard to solve within a reasonable time by using conventional computers.

7.3 Impact of Grid Structure and Topological Locations on System Strength

In order to overcome the challenge of identifying weakest combination of points of interconnection, a method is proposed based on analysis of impact of grid structure on the system strength. This method helps find the group of weakest buses/points of interconnection based on power grid structure in a timely manner.

This method is another application of SDSCR measure proposed in Chapter 3. By assuming that the voltages at all points of interconnection are equally maintained at the

desired point and all the renewable resources have equal generation capacities (i.e.,

$V_{R,i} = V_{R,j}$ and $P_{R,i} = P_{R,j}$), the SDSCR equation can be simplified as follows,

$$SDSCR_i = \frac{1}{\left| 1 + \sum_{j \in R, j \neq i} \frac{Z_{RR,ij}}{Z_{RR,ii}} \right| P_{R,i} |Z_{RR,ii}|} \quad (67)$$

As it can be seen in (66), the system strength at the point of interconnection i (i.e., $SDSCR_i$) is inversely proportional to the amount of renewable power generation at that point (i.e., $P_{R,i}$). The inversely proportional relation is weighted by several constant factors. Considering this fact, (66) can be rewritten as follows,

$$SDSCR_i = \frac{1}{w_i \times P_{R,i}} \quad (68)$$

where,

$$w_i = \frac{1}{\left| 1 + \sum_{j \in R, j \neq i} \frac{Z_{RR,ij}}{Z_{RR,ii}} \right| |Z_{RR,ii}|} \quad (69)$$

In (67), w_i is the weight for the amount of renewable power generation at the point of interconnection i that determines the system strength at that point. w_i is only comprised of structural related factors, which means it will be constant by variations in the operating condition of the power grid. It may only change by changing the location of renewable resources and/or the power grid structure, such as adding/upgrading a transmission line, transformer, etc. In w_i , the variables $Z_{RR,ij}$ and $Z_{RR,ii}$ are elements of the Z_{bus} matrix which show the electrical distance between the renewable resource j and the equivalent

AC power grid seen from point i , and the electrical distance between the renewable resource i and the equivalent AC power grid, respectively.

To take benefit of analyzing the grid structure and topological locations on system strength evaluation, (68) is needed to be more closely studied. For instance, if two solar PV plants are planned to be interconnected to a power grid⁸, under the aforementioned assumptions, the SDSCR is,

$$SDSCR_i = \frac{1}{\left| \frac{Z_{RR,ii}}{Z_{RR,ii}} + \frac{Z_{RR,ij}}{Z_{RR,ii}} \right| P_{R,i} |Z_{RR,ii}|} \quad (70)$$

Equation (69) shows the SDSCR measure for evaluating the system strength at the point of interconnection i in a power grid interconnected to two renewable resources. In this equation, $|Z_{RR,ii}|$ is a constant value related to the location of renewable resource connected to point i ; and it is electrical distance between the renewable resource i and the equivalent AC power grid. The ratios $\frac{Z_{RR,ii}}{Z_{RR,ii}}$ and $\frac{Z_{RR,ij}}{Z_{RR,ii}}$ in the denominator of (69) show the structural impact of renewable resources i and j on the system strength at the point of interconnection i , respectively. Thus, each of these two quantities can be used as an indicator for the significance of the impact each renewable resource may have on the system strength at point i .

They are both complex number; hence the structural impact of each renewable resource (j) on a point of interconnection of interest (i) can be written as follows,

⁸ In this example, only two renewable resources are considered for the sake of simplicity of illustration. Otherwise, a real-world large-scale power grid may be interconnected to hundreds of renewable resources, and the SDSCR can accurately evaluate the system strength at each point or interconnection.

$$\Gamma_j = \frac{Z_{ij}}{Z_{ii}} = |\Gamma_j| \angle \theta_{\Gamma_j} \quad (71)$$

where, Γ_j is the structural impact of each renewable resource (j) on a point of interconnection of interest, θ_{Γ_j} is the angle of Γ_j , and $|\Gamma_j|$ is the magnitude of Γ_j .

7.4 Identifying weakest combination of points of interconnection grid structure analysis

As each complex number introduces a vector, Γ_j is also a vector with certain magnitude and angle. To identifying weakest combination of points of interconnection, this property is used to determine integration or renewable resources to which group of buses can result in the lowest system strength.

It can be seen from (67)-(68), that obtaining the lowest system strength (SDSCR) at point of interconnection i requires maximum summation of the ratios in the denominator (i.e., $\Gamma_i, \dots, \Gamma_k$). As Γ_j 's are vectors, their summation is maximum if the angles among them are small and their magnitudes are large. In other words, the renewable resources associated with (Γ_j) vectors with the largest magnitudes that create the smallest angles with the vector associated with the point of interconnection of interest (Γ_i) will have the most significant impact on the system strength at point i .

To identify the weakest combination of points of interconnection, a Γ vector can be assigned to each candidate for integration of renewable resources. Then all the vectors can be compared and studied together to find a group of vectors that create the maximum summation of ratios in the denominator of (68).

To illustrate it, consider Figure 31 that shows the node-edge model of transmission system of a large-scale power grid. In this system, the dots and edges show the buses and the transmission lines respectively. Under current operating condition there a renewable resource is interconnected to the bus highlighted in red; and there are three candidates for integration of another new renewable resource (i.e., blue, green and purple buses).

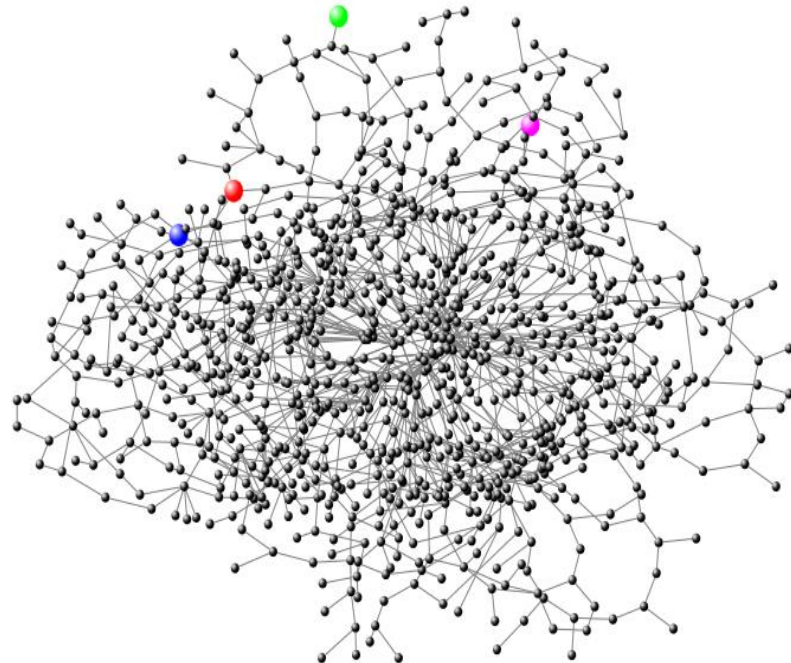


Figure 31. Node-edge model of transmission system of a large-scale power grid

In order to find the weakest combination of points of interconnection while a renewable resource is interconnected to the red bus, a vector (Γ) is assigned to each four points of interconnection. In the study, the goal is to identify which vector can create the biggest resultant vector with the vector associated with the red point. Creation of the biggest resultant vector requires having the smallest angle with the vector associated with the red bus with the biggest magnitude, as suggested by the vectors summation rule.

Figure 32 shows a plane including all the four vectors associated with the four points of interconnection. The color of each vector agrees with the color of the bus indicated in Figure 31.

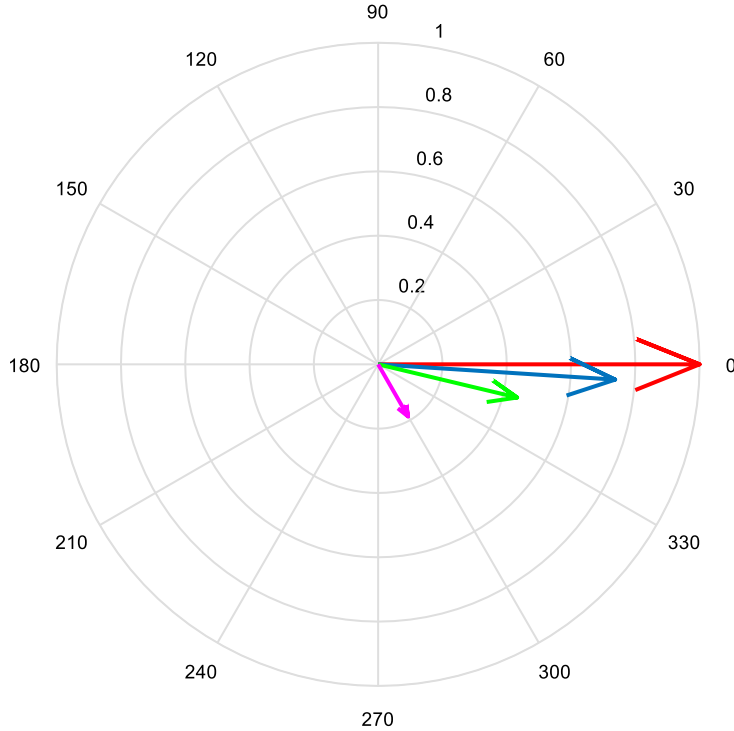


Figure 32. Plot of vectors associated with points of interconnection

In Figure 32, the red vector associated with the red point of interconnection is considered as the reference vector, and the status of other vectors will be evaluated with respect to it. It can be seen that the blue and the green vectors are bigger than the purple one and create smaller angles with the red vector. It implies that integration of a renewable resource to the purple bus will have the least impact on the system strength at the red point of interconnection. Since it will create the smallest resultant vector with the red vector, and consequently, the SDSCR will be maximized.

To identify the weakest combination of points of interconnection, it can be seen that among the blue, green and purple vectors, the blue vector is the biggest in term of

magnitude and creates the smallest angle with the reference vector (i.e., the red vector). Integration of a renewable resource to the blue bus will create the biggest resultant vector with the reference (red) vector, which means renewable generation at the blue bus will have the most impact on the system strength at the red point of interconnection. Thus, the weakest combination of points of interconnection in this system is the red and blue buses. As discussed before, another group of candidates for future integrations will result in different results due to structural characteristics of the power grid.

7.5 Criteria for identification of the weakest combination of points of interconnection based on grid structure

Based on the findings on grid structure analysis, a criterion is developed that can be used to identify the weakest combination of points of interconnection. The basis of the criterion is based on the following power grid structural impact analysis.

As shown in Figure 33, the vector associated with the reference bus in coincided on the horizontal axis with magnitude one and angle zero. Given this condition, if the angle of ratio ($\frac{Z_{RR,ij}}{Z_{RR,ii}}$) for point of interconnection j is smaller, the renewable resource at point of interconnection j has relatively more significant impact on system strength at point of interconnection i . Under this condition, when the angle of ratio ($\frac{Z_{RR,ij}}{Z_{RR,ii}}$) is in the quadrants II or III, the renewable resource at point of interconnection j has relatively less impact on system strength at point of interconnection i . The impact of other renewable generations on the system strength at the point of interconnection i is dependent on the resultant vector.

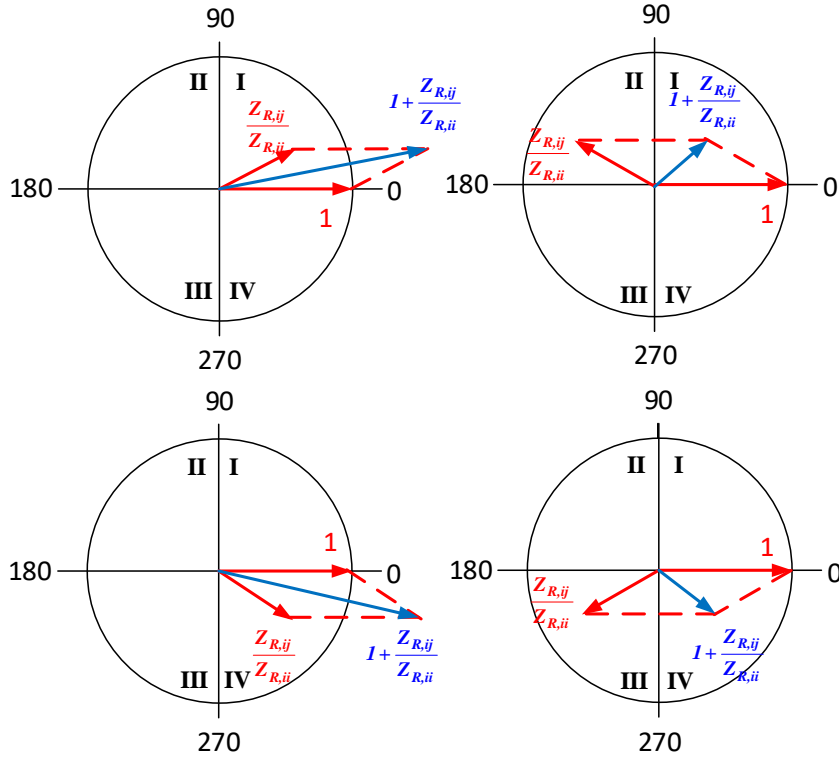


Figure 33. Structural impact on system strength (vector angle)

If angle of ratio $(\frac{Z_{RR,ij}}{Z_{RR,ii}})$ is smaller, renewable resource at point of interconnection j has relatively more significant impact on the system strength at point of interconnection i .

The impact of vectors magnitude is illustrated in Figure 34. For vectors located in quadrants I and IV, larger magnitude of ratio $(\frac{Z_{RR,ij}}{Z_{RR,ii}})$ means more significant impact of renewable resource at the point of interconnection j on the system strength at the point of interconnection i . For vectors located in quadrants II and III, smaller magnitude of ratio $(\frac{Z_{RR,ij}}{Z_{RR,ii}})$ means more significant impact of renewable resource at the point of interconnection j on the system strength at the point of interconnection i .

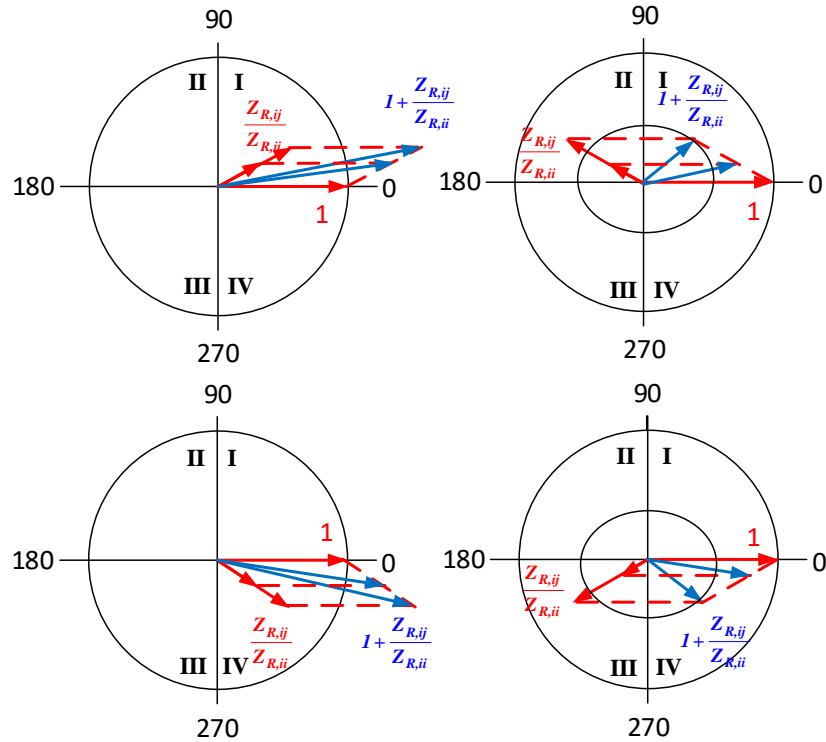


Figure 34. Structural impact on system strength (vector magnitude)

Based on the insights obtained from above structural analyses, the following criterion is developed for identification of the weakest combination of points of interconnection for integration of renewable resources,

- Criterion (a): For the points of interconnection with Γ_i vectors located in quadrants I and IV, weakest combination of points of interconnection are selected by ranking magnitudes of $(\frac{Z_{RR,ij}}{Z_{RR,ii}})$ in the ascending order.
- Criterion (b): For the points of interconnection with Γ_i vectors located in quadrants II and III, weakest combination of points of interconnection are selected by ranking angle of $(\frac{Z_{RR,ij}}{Z_{RR,ii}})$ in their ascending order.

Comparing the results obtained from exhaustive search shows that the developed criterion can precisely identify the weakest combination of points of interconnection. Figure 35 shows the recursive procedure for identifying weakest combination of points of interconnection.

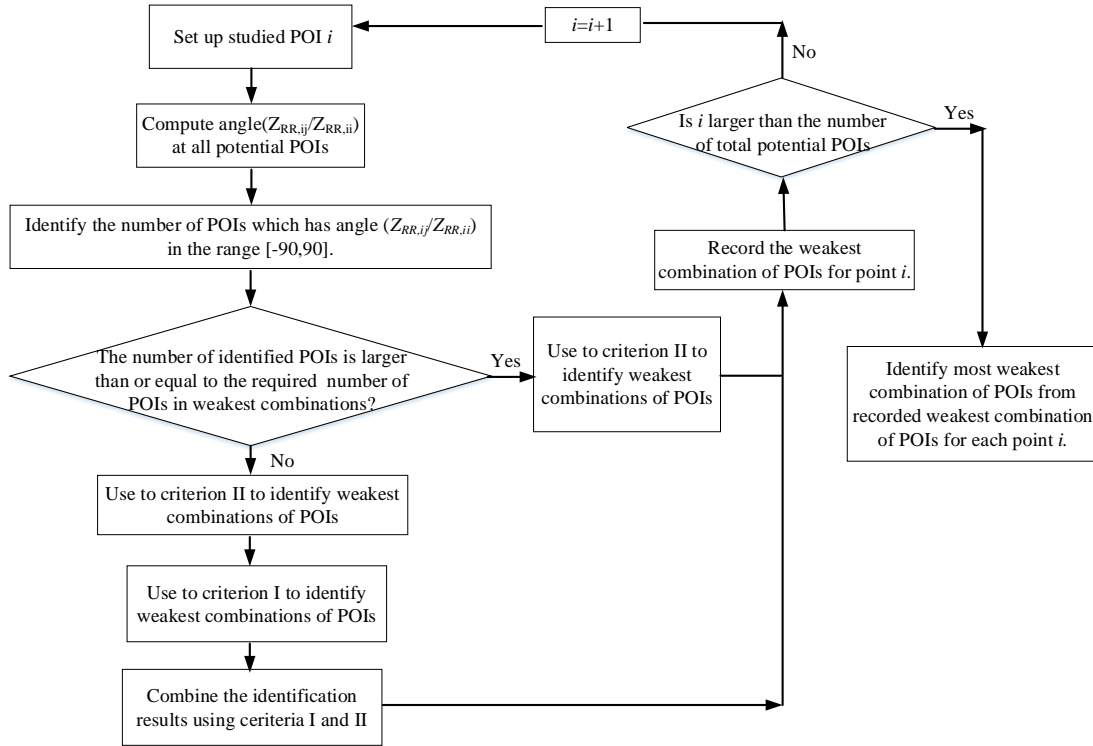


Figure 35. Flowchart of recursive procedure for identifying weakest combinations

Chapter 8: Simulation Studies

In this chapter, practical applicability and effectiveness of the proposed measure for system strength evaluation and other algorithms for better estimation of renewable power generation are presented. To this end, large-scale power grids and real-world wind power generation datasets are studied through several case studies and stressed scenarios.

8.1 SDSCR Measure Case Study

In order to illustrate the accuracy of system strength evaluation for integration of renewable energy resources using SDSCR measure, and demonstrate its privileges over the existing measures, the validity of the system strength evaluation results obtained from each measure (i.e., basic SCR, WSCR, CSCR and SDSCR) are investigated under a critical operating condition.

To this end a large-scale, real-world power grid is used for the simulation study. This study demonstrates the practical applicability of the SDSCR measure for evaluating the system strength at the points of interconnection of renewable resources in large-scale power grids with high penetration of renewable energy. An excerpt of this power grid is shown in Figure 36. This power grid is comprised of 5,700 buses, over 9,980 lines and transformers and 567 generation units. As it can be seen in Figure 36, this system is interconnected to three solar PV plants. The equivalent power generation capacities of the solar PV plants are shown in Table 5.

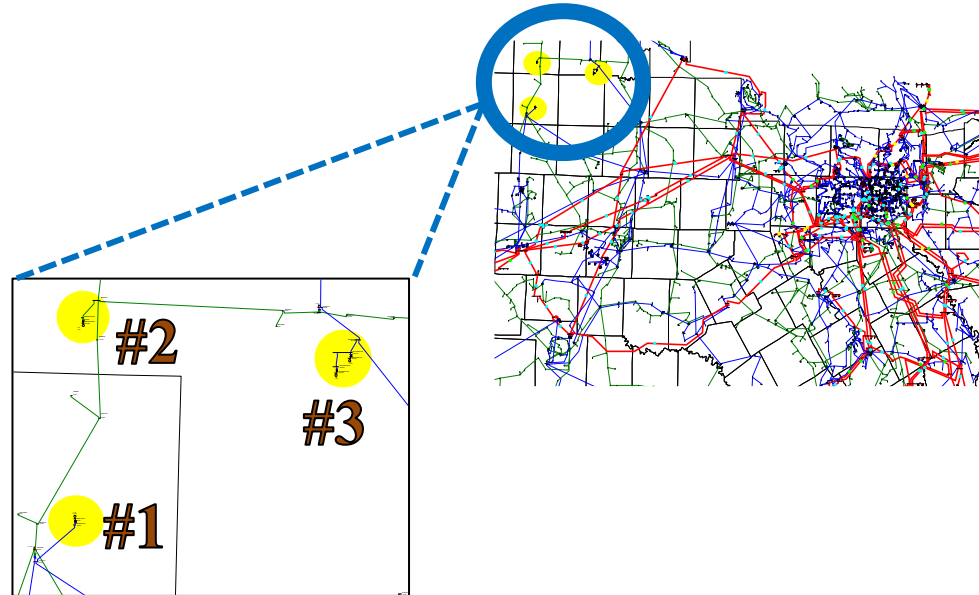


Figure 36. Excerpt of a large-scale power grid with three renewable resources

Table 5. Solar PV plants generation capacities

Solar PV Plant Number	Generation Capacity (MW)
1	45
2	93.3
3	46

This case study is a comprehensive simulation study that evaluates the system strength for a wide range of renewable power injection into the power grid. The focus of this study is mainly on the following items,

- Evaluating the system strength at the point of interconnection of renewable resource #1 while renewables #2 and #3 are generating at their nominal values.
- investigating the impact of significant variations in output of this solar PV plant on the system strength at the point of interconnection of the other 2 renewable resources.

- comparing the results of system strength evaluation from the 4 discussed measures to demonstrate the privilege of the proposed measure over the existing ones.

Having renewable resources #2 and #3 generating at their rated values, the output of renewable resource #1 is being increased in 10MW step sizes and the its associated P-V curve is calculated as shown in Figure 37. The P-V curve is used to set up the dispatch of renewable resource #1 for a range of 45MW to 185MW in 10MW step sizes (i.e., moving from rated value to the voltage instability operating point).

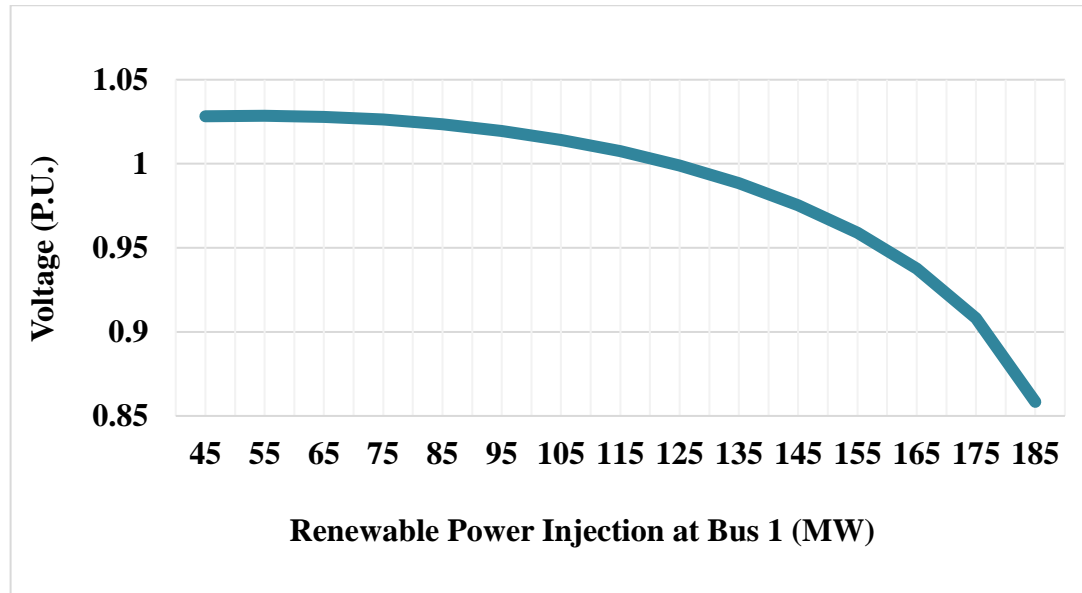


Figure 37. P-V Curve at bus interconnected to renewable resource #1

Then the system strength is evaluated for each operating condition using the 4 measures. The results of the systems strength evaluation using each measure is shown in Figure 38. In this Figure, the results obtain from using each measure is shown on a

horizontal axis by the blue arrow. The start of the arrow shows the normal operating condition and its tip shows the voltage collapse occurrence operating condition (i.e., knee point of P-V curve).

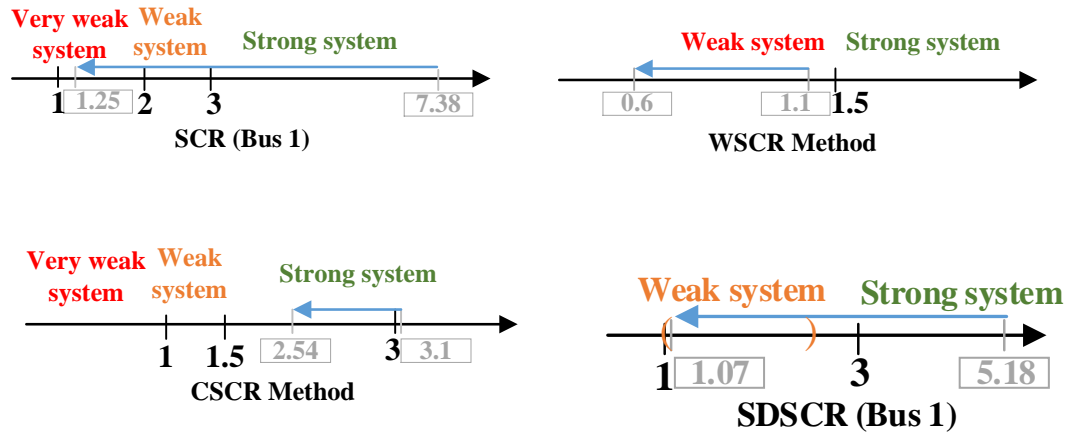


Figure 38. Results of system strength evaluation for POI #1

To confirm the validity of the results, obtained from each measure, the results are compared against the measures' criterion/threshold and the system realistic operating condition. As it can be seen in Figure 38, the SCR measure overestimates the system strength, which is expected. Since, it does not consider the interaction among the renewable resources. On the collapse point of the system that is the tip of the blue arrow the system strength is supposed to be equal to one, however, it is overestimated. The WSCR measure underestimates the system strength. Since based on its criterion, under normal operation condition, the system strength should be over 1.5; however, it is evaluated equal to 1.1. The CSCCR measure overestimates the system strength. Since based on its criterion, under critical operation condition, the system strength should be

below 1.5, which is not the case. It basically shows the system is strong when the renewable power generation at bus #1 is equal to the nose point of the PV curve. In addition, the CSSCR and WSCR measure are unable to uniquely evaluate the system strength at each point of interconnection. They only evaluate the system strength for the whole system that reduces the resolution of the results. The SDSCR accurately evaluates the system strength at this point of interconnection. Under normal operation condition, the system strength is identified as strong ($SDSCR = 5.18$), and under critical operating condition it identifies the system strength as very weak ($SDSCR = 1.07$).

In addition, the system strength is evaluated at the points of interconnection #2 and #3 using the four measures. Similar to the presentation of the results associated with the point of interconnection #1, these results are shown in Figure 39.

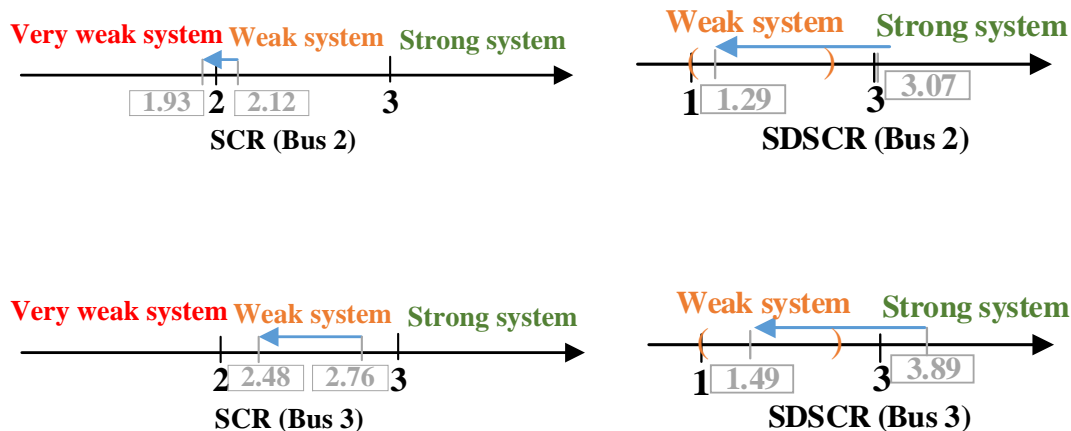


Figure 39. Results of system strength evaluation at POIs 2 and 3

The results of the CSCR and WSCR measures are identical to the results found for the point of interconnection #1. As it can be seen in Figure 39, at points of interconnection 2 and 3, the SCR measure does not consider the interaction among the

renewable resources and overestimates the system strength. The system strength at the voltage collapse point of bus #1 is supposed to be very close to 1 for buses #2 and #3, which is not the case. At the collapse point of the system (185 MW injection), the SCR shows system strength is fairly normal, the WSCR basically does not provide any particular information about the system strength, and the SDSCR shows weakness at the point of interconnection 2 and 3, that is not accurate. The SDSCR accurately evaluates the system strength at both points of interconnection. Under normal operation condition, the system strengths are identified as strong for both points of interconnection (3.07, 3.89), and under critical operating condition it identifies the system strength both points as weak (1.29 and 1.49).

This study on the large-scale power system confirms that,

- SCR,
 - It may overestimate the system strength.
 - It does not consider the interaction among the renewable resources.
- WSCR and CSCR,
 - They may not be able to accurately estimate the system strength.
 - They cannot explain the system strength in terms of voltage stability.
 - They cannot evaluate the system strength at each specific point of interconnection.
- SDSCR,
 - It can evaluate the system strength consistent system operation conditions.
 - It explains the system strength in terms of voltage stability.
 - It evaluates the system strength at each specific point of interconnection.

8.2 Wind Turbine Power Curve Estimation Case Study

In this section, practical applicability and effectiveness of the proposed algorithm is illustrated using a 5-minute time-series dataset of a wind turbine power generation and the corresponding wind speed. The dataset includes 12 months of the wind turbine operation data, with over 100,000 rows.

Following the procedure of the proposed algorithm as shown in Figure 20, the power curve from the 5-minute time-series dataset is estimated based on the following six major steps:

- As shown in Figure 18, the scatterplot is generated to visualize the dataset. It can be seen from this Figure that the raw data includes several outliers and a significant number of samples with $s_i = 0$, which do not provide useful information to construct the model for estimating the power curve. These samples as well as samples where $p_i < 0$ (negative generation) are mostly associated with those moments when wind speed is below the cut-in speed and the wind turbine consumes power to start operating. These points cause a noticeable bias in G that will be recursively reduced using our proposed algorithm.
- According to the scatterplot shown in Figure 18, the power curve with 3 linear line segments and the two break points is estimated. The piece-wise linear functions and the set of uncertain parameter θ are defined as follows,

$$p_L = \begin{cases} p_1 = b_1 s + a_1, & s < c_1 \\ p_2 = b_2 s + a_1 + (b_1 - b_2)c_1, & c_1 < s < c_2 \\ p_3 = b_3 s + a_1 + (b_1 - b_2)c_1 + (b_2 - b_3)c_2, & s > c_2 \end{cases} \quad (72)$$

$$\theta = \{b_1, a_1, b_2, c_1, c_2, b_3\} \quad (73)$$

- The initial values for these uncertain parameters in θ are approximately calculated, and then calculation results are used in the SAS non-linear parameter estimation procedure to obtain the best fitted values for the parameters in set θ .
- Following the parameter estimation, we create a new dataset (tmp) including the wind speed variable (s), and the values of p_1 , p_2 and p_3 over all ranges of s as variables (i.e., $tmp = \{p_L | p_i \text{ for all } s \text{ ranges}\}$). Using the dataset tmp the regression analysis is carried out and the predicted values of p_L (i.e., \bar{p}_L) are stored in tmp .
- \bar{p}_L will be used as a benchmark for outlier elimination. We select $\rho = 2$ to determine the symmetric interval (η) centered around \bar{p}_L with the length of 4 standard deviations of \bar{p}_L .
- After eliminating the outliers, the remaining observations will be stored in a new dataset (ω_1). At this stage, the algorithm repeats the steps for the second attempt starting from the non-linear parameter estimation for ω_1 to improve the model based on the cleaned dataset.

In this step, the estimated values for parameters in θ obtained in the first attempt (recursion number zero) will be used as initial values for recursion number 1. The algorithm completes the steps to generate ω_2 . Then, if it meets the convergence

criterion, the recursive process stops; otherwise, the algorithm iterates the steps for $\omega_2, \dots, \omega_k$ until it converges.

According to the major steps above, the algorithm converges after 7 attempts (6 recursions). Table 6 shows the results of iterative non-linear parameter estimation for the recursive outlier elimination. From this Table, it can be seen that for each recursion, the most updated dataset is used to improve the initial values until the convergence criterion is met. Table 7 shows the numbers of eliminated outliers during each recursion. According to this Table during the first attempt 1232 outliers are eliminated, which are mostly zero and negative observations. Then with more iterations, the number of eliminated outliers are decreases until no more outlier is eliminated during the 6th recursion. It means ω_5 associated with 5th recursion will be the final power curve dataset.

Table 6. Results of iterative non-linear parameter estimation for recursive outlier elimination

<i>Data Cleaning Results</i>	Recursion 0		Recursion 1		Recursion 2		Recursion 3		Recursion 4		Recursion 5		Recursion 6	
	Initial	Estim.	Initial	Estim.										
b_1	40	56.58	56.58	53.75	53.75	52.5	52.5	52.2	52.2	52.19	52.19	52.103	52.103	52.103
a_1	0	-123.1	-123.1	-114.9	-114.9	-111.5	-111.5	-110.7	-110.7	-110.4	-110.4	-110.3	-110.3	-110.3
c_1	5.3	5.99	5.99	5.73	5.73	5.68	5.68	5.66	5.66	5.66	5.66	5.66	5.66	5.66
c_2	11.5	11.77	11.77	11.57	11.57	11.56	11.56	11.55	11.55	11.55	11.55	11.56	11.56	11.56
b_2	211.7	216.6	216.6	222.9	222.9	222.8	222.8	222.7	222.7	222.73	222.73	222.7	222.7	222.7
b_3	-4.8	0.473	0.473	1.245	1.245	0.961	0.961	0.899	0.899	0.898	0.898	0.898	0.898	0.898
Assoc. Dataset	G		ω_1		ω_2		ω_3		ω_4		ω_5		N/A (converged)	

Table 7. Number of eliminated outliers in each recursion

Recursion Number	Number of Eliminated Observations
Recursion 0	1232
Recursion 1	685
Recursion 2	241
Recursion 3	78
Recursion 4	21
Recursion 5	3
Recursion 6	0

Figure 40 shows the power curves after the first recursion, and Figure 41 shows the power curves after the second recursion. These two Figures show how the algorithm cleans the wind speed-wind power generation dataset recursively. It can be seen from Figure 40 and Figure 41 that after the first two recursions most of outliers are eliminated; thus, the bias is reduced compared to those from the raw dataset as shown in Figure 18. Comparing Figure 18 and Figure 42, it can be seen that the outliers in that raw data shown in Figure 18 are effectively eliminated in the final dataset; the observations associated with zero generation are also eliminated using a scientific technique.

This dataset and the associated piece-wise linear model obtained from the last recursion will be beneficial for different operation assessment purposes. Utilizing the algorithm to reduce the bias for this particular wind turbine could effectively avoid overestimating/underestimating the wind power generation.

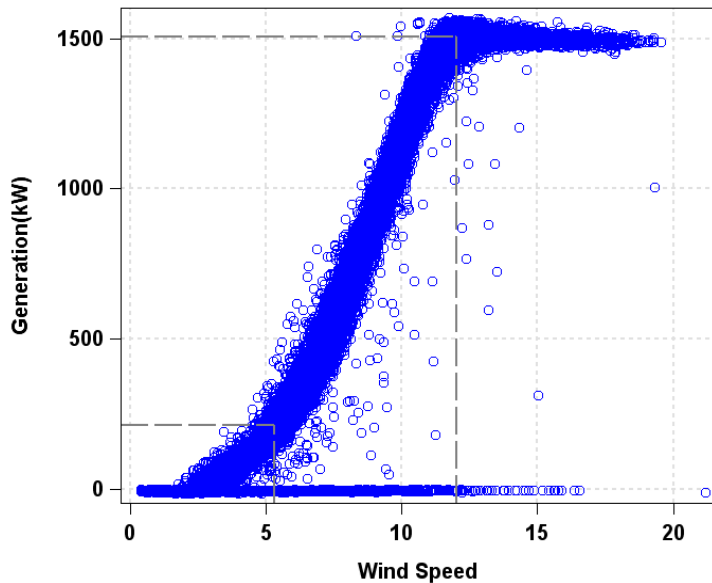


Figure 40. Power curver after first recursion

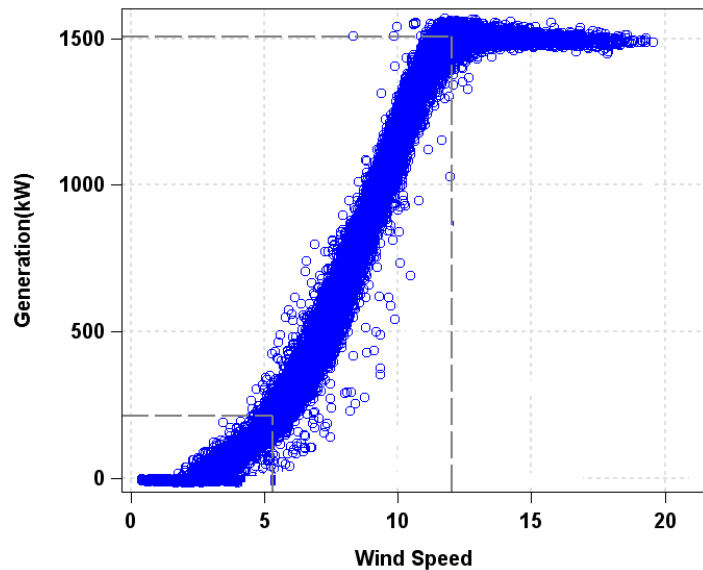


Figure 41. Power curve after second recursion

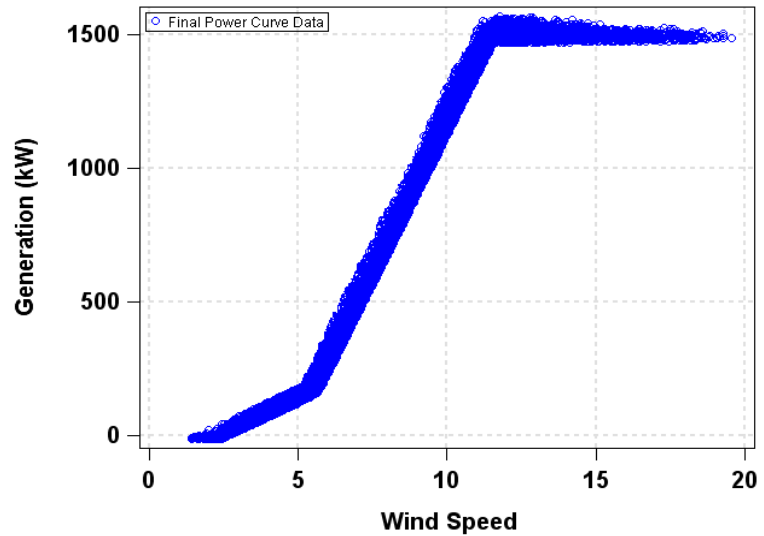


Figure 42. Final power curve piece-wise linear model

Summary and Concluding Remarks

In this dissertation, a new measure is proposed for evaluating the strength of a power grid with the high penetration of renewable resources. Compared to Short Circuit Ratio (SCR), Weighted Short Circuit Ratio (WSCR) and Composite Short Circuit Ratio (CSCR), the proposed Site Dependent Short Circuit Ratio (SDSCR) has the following advantages: 1) it can quantifies the system strength in terms of the distance to static voltage stability limit; 2) it can take into account the effect of the interaction among renewable generation resources; 3) it can provide information about the system strength at each individual point of interconnection of renewable resources; and 4) it was showed that the commonly used SCR is the special case of the SDSCR.

The proposed measure evaluates the system strength based on the power grid structural characteristics and considering the amount of renewable power generation at a point of interconnection. It can be used for various studies concerning system strength evaluation, such as identifying weakest combination of points of interconnection. As another application of the proposed measure, an approach is developed to identify the weakest combination of points of interconnection through structural analysis.

In order to improve the system strength evaluation studies using the proposed measure, this dissertation also proposed an algorithm for more accurate estimation of wind power generation, and an approach for estimation of solar PV power generation drops.

For more accurate estimation of wind power generation, A SAS-based algorithm is proposed to estimate power curves using the actual dataset of wind power generation and wind speed while simultaneously minimizing both the modeling and bias errors caused

by outliers in the dataset. In the algorithm, a continuously updated piece-wise linear model is used to minimize modeling errors while bias errors are reduced by using SAS software package to recursively clean outliers out in the real dataset. As a result of being SAS-based, the algorithm is designed to be self-adaptive, which makes it applicable to a variety of datasets including any kind of bias or undesirable observations. In addition to power curves, the proposed algorithm can also provide cleaned dataset and the associated piece-wise linear model for various operation assessment purposes, such as efficiency and fatigue analysis studies. The effectiveness and practical application of the proposed algorithm is demonstrated through a real-world case study.

In the future research, the proposed algorithm will be utilized to study the wind turbine fatigue based on changes of the average power curve over years of operation, aiming at improving the power curve based forecasting of wind power outputs and screening the turbines that might have some defects. Moreover, we would like to investigate the wind turbine performance under various weather conditions (e.g., wind direction, relative humidity and air pressure). The outcome of these researches may be beneficial for wind farms and power system operators.

For estimation of solar PV power generation drops, an approach is developed to forecast the clouds distribution using historical weather data. The approach utilizes a time-series dataset including several weather parameters around the solar PV plant of interest. This dataset is used to train and validate an Artificial Neural Network (ANN) model that forecasts the solar irradiance/clouds distribution based on the weather parameters. Given a big dataset including all the important weather parameters as the input of the ANN model, it's expected that the model can precisely forecast the solar irradiance. However,

an important missing parameter in the ANN model input dataset imposes an error in the solar irradiance forecast results. The weather scientists believe that the missing parameter is the cloud information. In other words, existence of clouds cause forecasting error in the ANN model output. Thus, it can be assumed that the forecasting error of solar irradiance forecast using a ANN model at each time interval is caused by the clouds at that time interval. Hence, the approach considers the ANN model's solar irradiance forecast error as an indication of cloud information. As the shape/sparseness of clouds includes a high degree of uncertainty, this approach identifies the status of clouds in terms of various modes. This way, significant changes in clouds distribution can be identified based on change of clouds mode from one to the other.

References

- [1] S.-H. (Fred) Huang, “System Strength Discussion,” *ERCOT*.
- [2] S. H. Huang, J. Schmall, J. Conto, J. Adams, Y. Zhang, and C. Carter, “Voltage control challenges on weak grids with high penetration of wind generation: ERCOT experience,” *IEEE Power Energy Soc. Gen. Meet.*, pp. 1–7, 2012.
- [3] “NERC Essential Reliability Services Task Force: Measures Framework Report,” *NERC*. [Online]. Available: [http://www.nerc.com/comm/Other/essntlrlbltysrvcstskfrcDL/ERSTF Framework Report - Final.pdf](http://www.nerc.com/comm/Other/essntlrlbltysrvcstskfrcDL/ERSTF%20Framework%20Report%20-%20Final.pdf). [Accessed: 01-Jan-2015].
- [4] L. Wang, C. J. Yeh, M. H. Hsieh, C. T. Wu, and C. L. Lu, “System-impact analysis of a large-scale offshore wind farm connected to Taiwan power system,” *Conf. Rec. - IAS Annu. Meet. (IEEE Ind. Appl. Soc.)*, pp. 1–5, 2013.
- [5] P. Kundur, *Power System Stability and Control*. Toronto, ON, CA: EPRI, 1993.
- [6] “IEEE Guide for Planning DC Links Terminating at AC Locations Having Low Short-Circuit Capacities, IEEE Std 1204-1997,” 1997.
- [7] H. Urdal, D. Rostom, A. Dahresobh, C. Ivanov, J. Zhu, and R. Ierna, “System strength considerations in a converter dominated power system,” *IET Renew. Power Gener.*, vol. 9, no. 1, pp. 10–17, 2015.
- [8] S. L. Lorenzen, A. B. Nielsen, and L. Bede, “Control of A Grid Connected Converter During Weak Grid Conditions.”
- [9] A. Gavrilovic, “ACDC system strength as indicated by short circuit ratios,” *IET, Int. Conf. AC DC Power Transm.*, pp. 27–32, 1991.
- [10] GE and MISO, “GE Energy Consulting: Minnesota Renewable Energy

Integration and Transmission Study (Final Report).” [Online]. Available: <http://mn.gov/commerce-stat/pdfs/mrits-report-2014.pdf>.

[11] R. Achilles and S. MacDowell, “GE Energy Consulting: Report to NERC ERSTF for Composite Short Circuit Ratio (CSCR) Estimation Guideline,” 2015.

[12] J. Schmall, S. H. Huang, Y. Li, J. Billo, J. Conto, and Z. Yang, “Voltage stability of large-scale wind plants integrated in weak networks: An ERCOT case study,” *IEEE Power Energy Soc. Gen. Meet.*, vol. 2015–Septe, 2015.

[13] Y. Zhang, S.-H. F. Huang, J. Schmall, J. Conto, J. Billo, and E. Rehman, “Evaluating system strength for large-scale wind plant integration,” *2014 IEEE PES Gen. Meet. / Conf. Expo.*, pp. 1–5, 2014.

[14] “Comprehensive Large Array-data Stewardship System (NOAA).” [Online]. Available:

https://www.nsof.class.noaa.gov/saa/products/search?datatype_family=GVAR_IMG.

[15] “National Weather Center - The University of Oklahoma.” [Online]. Available: <http://www.ou.edu/nwc.html>.

[16] A. M. Gole and J. Z. Zhou, “VSC transmission limitations imposed by AC system strength and AC impedance characteristics,” *10th IET Int. Conf. AC DC Power Transm. (ACDC 2012)*, no. 2, pp. 06–06, 2012.

[17] J. Chen-chen, W. Jun, and B. Xiao-yu, “STUDY OF THE EFFECT OF AC SYSTEM STRENGTH ON THE HVDC STARTUP CHARACTERISTICS,” no. 1, pp. 3–7.

[18] Y. Wang, X. Li, C. Wen, and Y. He, “Impact of AC system strength on commutation failure at HVDC inverter station,” *Asia-Pacific Power Energy Eng. Conf.*

APPEEC, no. 51037003, pp. 2–5, 2012.

- [19] E. D. Crainic, X. D. Do, D. Mukhedkar, and H. P. Horisberger, “Power network observability: The assessment of the measurement system strength,” *IEEE Trans. Power Syst.*, vol. 5, no. 4, pp. 1267–1285, 1990.
- [20] S. I. Arman, R. Karki, and R. Billinton, “Resource Strength and Location Impact of Wind Power on Bulk Electric System Reliability,” 2016.
- [21] M. Javadi, B. Zhao, D. Wu, Z. Hu, and J. N. Jiang, “A Study of Reactive Power Margins in Power System Following Severe Generation Imbalance,” pp. 1–5, 2015.
- [22] M. Javadi, M. Hong, R. N. Angarita, S. H. Hosseini, and J. N. Jiang, “Identification of Simultaneously Congested Transmission Lines in Power Systems Operation and Market Analysis,” *IEEE Trans. Power Syst.*, vol. 8950, no. c, pp. 1–1, 2016.
- [23] A. S. Dobakhshari and M. Fotuhi-Firuzabad, “A Reliability Model of Large Wind Farms for Power System Adequacy Studies,” *Energy Conversion, IEEE Trans.*, vol. 24, no. 3, pp. 792–801, 2009.
- [24] R. Karki, P. Hu, and R. Billinton, “A simplified wind power generation model for reliability evaluation,” *IEEE Trans. Energy Convers.*, vol. 21, no. 2, pp. 533–540, 2006.
- [25] F. Vallee, J. Lobry, and O. Deblecker, “Impact of the wind geographical correlation level for reliability studies,” *IEEE Trans. Power Syst.*, vol. 22, no. 4, pp. 2232–2239, 2007.
- [26] I. F. MacGill, “Impacts and best practices of large-scale wind power integration into electricity markets Some Australian perspectives,” *IEEE Power Energy Soc. Gen. Meet.*, pp. 1–6, 2012.

- [27] Y. Zhang, A. Chowdhury, and D. O. Koval, “Probabilistic Wind Energy Modeling in Electric Generation System Reliability Assessment,” *Ind. Commer. Power Syst. Tech. Conf. IampCPS 2010 IEEE*, vol. 47, no. 3, pp. 1507–1514, 2010.
- [28] Y. Zhang and A. A. Chowdhury, “Reliability assessment of wind integration in operating and planning of generation systems,” *2009 IEEE Power Energy Soc. Gen. Meet.*, pp. 1–7, 2009.
- [29] M. Ghofrani, A. Arabali, M. Etezadi-Amoli, and M. S. Fadali, “Energy storage application for performance enhancement of wind integration,” *IEEE Trans. Power Syst.*, vol. 28, no. 4, pp. 4803–4811, 2013.
- [30] M. Schlechtingen, I. F. Santos, and S. Achiche, “Using data-mining approaches for wind turbine power curve monitoring: A comparative study,” *IEEE Trans. Sustain. Energy*, vol. 4, no. 3, pp. 671–679, 2013.
- [31] B. P. Hayes, I. Ilie, a. Porpodas, S. Z. Djokic, and G. Chicco, “Equivalent power curve model of a wind farm based on field measurement data,” *2011 IEEE Trondheim PowerTech*, pp. 1–7, 2011.
- [32] M. Lydia, A. I. Selvakumar, S. S. Kumar, and G. E. P. Kumar, “Advanced algorithms for wind turbine power curve modeling,” *IEEE Trans. Sustain. Energy*, vol. 4, no. 3, pp. 827–835, 2013.
- [33] C. Wei and P. Yue, “Calibration Power Curve of Wind Generator and Forecasting Model of Wind Power Unit,” in *Proceeding of the 2015 IEEE International Conference on Information and Automation*, 2015, pp. 583–587.
- [34] J. Park, J. Lee, K. Oh, and J. Lee, “Development of a Novel Power Curve Monitoring Method for Wind Turbines and Its Field Tests,” *IEEE Trans. Energy*

Convers., vol. 29, no. 1, pp. 119–128, 2014.

- [35] A. Goudarzi, S. Member, I. E. Davidson, S. Member, G. K. Venayagamoorthy, and S. Member, “Intelligent Analysis of Wind Turbine Power Curve Models,” in *Symposium on Computational Intelligence Applications in Smart Grid (CIASG), IEEE*, 2014, pp. 1–5.
- [36] A. Kusiak, H. Zheng, and Z. Song, “On-line monitoring of power curves,” *J. Renew. Energy*, vol. 34, no. 6, pp. 1487–1493, 2009.
- [37] J. Zhou, P. Guo, and X. Wang, “Modeling of Wind Turbine Power Curve Based on Gaussian Process,” in *Proceedings of the 2014 International Conference on Machine Learning and Cybernetics*, 2014, pp. 13–16.
- [38] M. H. Zamani, G. H. Riahy, and A. J. Ardakani, “Modifying power curve of variable speed wind turbines by performance evaluation of pitch-angle and rotor speed controllers,” *2007 IEEE Canada Electr. Power Conf. EPC 2007*, pp. 347–352, 2007.
- [39] S. H. Jangamshetti and V. Guruprasada Rau, “Normalized power curves as a tool for identification of optimum wind turbine generator parameters,” *IEEE Trans. Energy Convers.*, vol. 16, no. 3, pp. 283–288, 2001.
- [40] T. Jin and Z. Tian, “Uncertainty analysis for wind energy production with dynamic power curves,” *2010 IEEE 11th Int. Conf. Probabilistic Methods Appl. to Power Syst.*, pp. 745–750, 2010.
- [41] S. Shokrzadeh, M. Jozani, and E. Bibeau, “Wind Turbine Power Curve Modeling Using Advanced Parametric and Nonparametric Methods,” *IEEE Trans. Sustain. Energy*, vol. 5, no. 4, pp. 1262–1269, 2014.
- [42] M. S. M. Raj, M. Alexander, and M. Lydia, “Modeling of wind turbine power

curve,” *Innov. Smart Grid Technol. - India (ISGT India), 2011 IEEE PES*, pp. 144–148, 2011.

[43] S. Z. Djokic, B. P. Hayes, R. Langella, and A. Tesa, “Modeling of Wind Farm Energy Resources and Wind Power Outputs Using Nested Markov Chain Approach,” *Int. Clean Electr. Power*, pp. 241–246, 2015.

[44] S. Gill, B. Stephen, and S. Galloway, “Wind turbine condition assessment through power curve copula modeling,” *IEEE Trans. Sustain. Energy*, vol. 3, no. 1, pp. 94–101, 2012.

[45] B. Stephen, S. J. Galloway, D. McMillan, D. C. Hill, and D. G. Infield, “A Copula Model of Wind Turbine Performance,” *Power Syst. IEEE Trans.*, vol. 26, no. 2, pp. 965–966, 2011.

[46] R. Cody, *Learning SAS by Example (A Programmer’s Guide)*. Cary, NC, USA: SAS Institute Inc., 2007.

[47] L. Ljung, *System Identification: Theory for the User*, 2nd ed. Prentice Hall, 1999.

[48] C. Almgren and G. Collins, “Solar PV Cells Free Electricity from the Sun?,” *Colorado State University*, 2016. [Online]. Available: https://www.engr.colostate.edu/ECE461/illustrative_presentation.pdf.

[49] “National Renewable Energy Laboratory (NREL).” [Online]. Available: <https://www.nrel.gov/csp/>.

[50] F. Giraud and M. Salameh, “Analysis of the Effects of a Passing Cloud on a Grid-Interactive Photovoltaic System with Battery Storage using Neural Networks,” *IEEE Trans. Energy Convers.*, vol. 14, no. 4, pp. 1572–1577, 1999.

[51] T. Verma, A. P. S. Tiwana, C. C. Reddy, V. Arora, and P. Devanand, “Data

Analysis to Generate Models Based on Neural Network and Regression for Solar Power Generation Forecasting,” *7th Int. Conf. Intell. Syst. Model. Simul.*, pp. 97–100, 2016.

- [52] W. Jewell and R. Ramakumar, “The effects of moving clouds on electric utilities with dispersed photovoltaic generation,” *IEEE Trans. Energy Convers.*, vol. EC-2, no. 4, pp. 570–576, 1987.